

1 **Short title:** Circadian clock regulates photoperiodic growth

2 Corresponding author details:

3 Lei Wang, Key Laboratory of Plant Molecular Physiology, CAS Center for Excellence in

4 Molecular Plant Sciences, Institute of Botany, Chinese Academy of Sciences. E-mail:

5 wanglei@ibcas.ac.cn (L.W.)

6

7 **Pseudo Response Regulators regulate photoperiodic hypocotyl growth by**
8 **repressing *PIF4/5* transcription**

9

10 **Na Li^{a,b,1}, Yuanyuan Zhang^{a,1}, Yuqing He^{a,b}, Yan Wang^{a,b} and Lei Wang^{a,b,*}**

11 ^a Key Laboratory of Plant Molecular Physiology, CAS Center for Excellence in Molecular
12 Plant Sciences, Institute of Botany, Chinese Academy of Sciences, Beijing 100093, China.

13 ^b University of Chinese Academy of Sciences, Beijing 100049, China.

14 ¹ N.L. and Y.Y.Z. contributed equally to this work.

15 * Corresponding author

16 **One-sentence summary:** Pseudo Response Regulator proteins and the Evening Complex
17 transmit daylength information to regulate photoperiodic hypocotyl growth by directly
18 repressing transcription of key growth regulators.

19 **Author contributions:** N. L., Y. Z. and Y. H. performed the experiments. N. L., Y.Z. and L.W.
20 designed the project, analyzed the data and wrote the article. L.W. agrees to serve as the author
21 responsible for contact and ensures communication.

22 **Funding information:** The work was supported by the Strategic Priority Research Program of
23 the Chinese Academy of Sciences, Grant No. XDB27030206, and the National Natural
24 Sciences Foundation of China (31670290 and 31570292) to L.W. Youth Innovation Promotion
25 Association CAS to Y. Z. (NO.2017110).

27 **Abstract**

28 The circadian clock measures and conveys daylength information to control rhythmic hypocotyl growth in
29 photoperiodic conditions to achieve optimal fitness, but it operates through largely unknown mechanisms.
30 Here, we show that Pseudo Response Regulators (PRRs) coordinate with the Evening Complex (EC), a
31 transcriptional repressor complex within clock core oscillator, to specifically regulate photoperiodic
32 hypocotyl growth in *Arabidopsis thaliana*. Intriguingly, a distinct daylength could shift the expression
33 phase and extend the expression duration of PRRs. Multiple lines of evidence further demonstrated that
34 PRRs directly bound the promoters of *PHYTOCHROME-INTERACTING FACTOR4* (*PIF4*) and *PIF5* to repress
35 their expression, hence PRRs act as transcriptional repressors of the positive growth regulators *PIF4* and
36 *PIF5*. Importantly, mutation or truncation of the TIMING OF CAB EXPRESSION 1 (TOC1) DNA binding
37 domain, without compromising its physical interaction with PIFs, still caused long hypocotyl growth under
38 short days, highlighting the essential role of the PRRs-PIFs transcriptional module in photoperiodic
39 hypocotyl growth. Finally, genetic analyses demonstrated that *PIF4* and *PIF5* are epistatic to *PRRs* in the
40 regulation of photoperiodic hypocotyl growth. Collectively, we propose that, upon perceiving daylength
41 information, PRRs cooperate with EC to directly repress *PIF4* and *PIF5* transcription together with their
42 post-translational regulation on PIFs activities, thus forming a complex regulatory network to mediate
43 circadian clock-regulated photoperiodic growth.

44

45 **Introduction**

46 Seedlings of terrestrial flowering plants display diel rhythmic growth upon responding to
47 recurring natural stimuli immediately after protruding from the soil. The photoperiod, i.e., the
48 daylength, is the most prominent environmental factor that shapes plant architecture and
49 determines growth phase transition. Photoperiod information, which reflects seasonal changes,
50 can be processed by circadian clock-dependent mechanisms to shape the gene expression
51 pattern, with an acrophase at a specific time of the day, thus to modulate a wide range of plant
52 growth and developmental processes, including flowering time (Yanovsky and Kay, 2002;
53 Valverde et al., 2004; Sawa et al., 2007; Sawa and Kay, 2011; Andres and Coupland, 2012; Lee
54 et al., 2017). In particular, the seedling hypocotyl displays robust growth rhythms under certain
55 photoperiodic conditions. The length of the hypocotyl is reversely associated with daylength,
56 which has long been considered as a coordinative mechanism between the circadian clock and
57 daily photoreception (Nozue et al., 2007; Niwa et al., 2009; Nomoto et al., 2012). Nevertheless,
58 the regulatory network underlying this coordinative mechanism is largely unknown.

59 Phytochrome-interacting factors (PIFs), a group of basic helix–loop–helix transcription
60 factors (Huq and Quail, 2002), can profile the hypocotyl photoperiodic growth dynamics, and
61 are regarded as converging regulators to explain the coincidence between external
62 environmental cues and the circadian clock (Millar, 2016; Quint et al., 2016). Under
63 photoperiodic conditions, the protein abundance and activity of *PIFs*, especially of *PIF4* and
64 *PIF5*, are concurrently regulated by light signaling and the circadian clock via a combination of
65 transcriptional and post-transcriptional mechanisms (Fujimori et al., 2004; Shen et al., 2007;
66 Nusinow et al., 2011; Nakamichi et al., 2012; Nieto et al., 2015; Soy et al., 2016; Zhu et al.,
67 2016; Martin et al., 2018). Light signals modulate PIF protein abundance by triggering physical
68 interaction between PIFs and phytochromes and subsequent degradation of PIFs (Al-Sady et
69 al., 2006; Shen et al., 2007), while the circadian clock mainly shapes the circadian
70 transcriptional waves of *PIF4* and *PIF5* (Nusinow et al., 2011; Nakamichi et al., 2012; Nieto et
71 al., 2015; Soy et al., 2016; Zhu et al., 2016; Martin et al., 2018). Thus, the diurnal regulation of
72 *PIF4* and *PIF5* transcription plays a critical role in photoperiodic hypocotyl cell elongation.

73 The circadian clock Evening Complex (EC), which is composed of EARLY FLOWERING 4
74 (ELF4), EARLY FLOWERING 3 (ELF3), and LUX ARRHYTHMO (LUX), inhibits *PIF4*
75 and *PIF5* expression in the early evening and the first part of night, thus directly allowing the
76 circadian clock to diurnally regulate hypocotyl growth (Nusinow et al., 2011). As the
77 transcriptional peak phase of *PIF5* is ahead of *PIF4* for about 2–4 h, when EC proteins have not
78 yet highly accumulated, it raises a possibility that other clock components are also involved in
79 the progressive repression of *PIF4* and *PIF5*. Hence, the intricate regulation of *PIF4* and *PIF5*
80 transcription remains to be fully unraveled (Nusinow et al., 2011; Nakamichi et al., 2012; Liu et
81 al., 2013; Liu et al., 2016; Zhu et al., 2016; Martin et al., 2018).

82 The *Arabidopsis thaliana* Pseudo Response Regulator (PRR) gene family is composed of
83 five members (*PRR9*, *PRR7*, *PRR5*, *PRR3*, and *TIMING OF CAB EXPRESSION 1 (TOC1)*),
84 each of which peaks at a specific time of day in a consecutive manner from dawn to dusk
85 (Matsushika et al., 2000; Nakamichi et al., 2010). PRR proteins were proposed to regulate
86 photoperiodic hypocotyl elongation mainly via two pathways. One is the transcriptional
87 regulation of *PIF4* and *PIF5* by *PRR5* and *PRR7* (Liu et al., 2013; Nakamichi et al., 2012), and
88 the other is the transcriptional activation activities of PIFs which are tightly regulated by the
89 circadian clock via physical interaction between PIFs and PRRs (Soy et al., 2016; Zhu et al.,
90 2016; Martin et al., 2018). Currently, the underlying mechanisms of the long hypocotyl
91 phenotype of *prp* mutants in short-day (SD) conditions or in response to temperature are
92 thought to be mainly due to their post-transcriptional regulation of PIFs via physical
93 interactions and antagonistically with PIFs by binding to a set of co-targets, including
94 *PHYTOCHROME INTERACTING FACTOR 3-LIKE 1 (PIL1)*, *YUCCA 8 (YUC8)*, and
95 *CYCLING DOF FACTOR 5 (CDF5)* (Martin et al., 2018; Soy et al., 2016; Zhu et al., 2016). In
96 addition, *TOC1* can physically interact with *ELF3* (Huang et al., 2016), the bridging protein
97 among EC, but it is still unclear whether *ELF3* and *TOC1* work in the same pathway or
98 independently to regulate photoperiodic hypocotyl growth. Moreover, how PRRs respond to
99 distinct daylength information at the transcriptional and post-transcriptional level and

100 subsequently transmit photoperiod information to control hypocotyl cell elongation is still
101 largely unknown.

102 Here, we show that PRRs and EC act additively in regulating photoperiodic hypocotyl
103 growth in Arabidopsis, and daylength information can alter the expression phase and duration
104 of PRRs. We further unveiled *PIF4* and *PIF5* as direct transcriptional targets of PRRs, and their
105 transcriptional patterns were accordingly altered by daylength information via PRRs.

106 Importantly, by using TOC1 DNA binding domain mutation or truncation alleles, we show that
107 the PRRs-*PIF*s transcription module is essential for regulating hypocotyl growth in
108 photoperiodic conditions. Together with the post-translational regulation of PIF abundance and
109 activities by PRRs and EC, we thus propose a complex regulatory network that mediates
110 circadian clock-regulated photoperiodic hypocotyl growth, by a combinatorial transcriptional
111 and post-transcriptional mechanisms.

112 **Results**

113 **PRRs Act Additively with EC to Regulate Photoperiodic Hypocotyl Growth**

114 Both PRRs and EC are involved in hypocotyl growth regulation (Sato et al., 2002;
115 Kaczorowski and Quail, 2003; Yamamoto et al., 2003; Nusinow et al., 2011; Nieto et al., 2015;
116 Soy et al., 2016; Zhu et al., 2016; Martin et al., 2018, Li et al., 2019). TOC1, the founding
117 member of PRRs, can physically interact with an EC component ELF3 (Huang et al., 2016).
118 Nevertheless, the relationship between PRRs and EC in regulating hypocotyl growth,
119 especially under photoperiodic conditions, is unclear. To systematically address this question,
120 we generated higher order Arabidopsis mutants between PRRs and EC components. After
121 growth for 5 days at different conditions, we measured the hypocotyl length and found that
122 *toc1*, *prr5*, *toc1 prr5*, and *elf3* mutants displayed dramatically longer hypocotyl phenotypes
123 under both short-day (SD, 8 h light / 6 h dark) and long-day (LD, 16 h light / 8 h dark)
124 conditions relative to Col-0, but not under constant light (LL) conditions (Figure 1A-1F).
125 Strikingly, the hypocotyls of *toc1 elf3* and *prr5 elf3* double mutants were significantly longer
126 than those of the single mutants, suggesting that they act additively to regulate hypocotyl

127 growth only under photoperiod conditions. Notably, the hypocotyl lengths of the *toc1 prr5 elf3*
128 triple mutant were modestly but significantly longer than those of the *toc1 prr5* and *elf3*
129 mutants under both LD and SD conditions ((Fig. 1A-1D), further supporting the notion that
130 PRRs and EC additively regulate hypocotyl growth. Since ELF3 has been shown to interact
131 with PIF4 to regulate hypocotyl growth independent of EC (Nieto et al., 2015), we further
132 examined the genetic relationship between PRRs and EC by using LUX, a DNA binding
133 protein in EC (Hazen et al., 2005; Nusinow et al., 2011). Consistently, the *toc1 prr5 lux* triple
134 mutant displayed significantly longer hypocotyls than either the *toc1 prr5* or *lux* mutants, in
135 both SD and LD conditions (Supplemental Fig. S1), further confirming that PRRs and EC
136 additively regulate photoperiodic hypocotyl growth. In addition, the transcript phases of *PRR9*
137 and *PRR7* displayed an inverse pattern to that of EC, but the hypocotyls of the *prp7 prp9* double
138 mutant were significantly longer than that of Col-0 (Nakamichi et al., 2005), specifically under
139 photoperiodic conditions, but not in constant light (Supplemental Fig. S2). Altogether, multiple
140 lines of genetic evidence clearly demonstrated that PRRs act additively with EC to regulate
141 hypocotyl growth under photoperiodic conditions.

142 **Daylength Information Alters the Expression Patterns of PRRs and EC**

143 In general, the hypocotyl length decreases with increasing daylength. However, the ratio of
144 hypocotyl length in SD vs. LD conditions was significantly increased in the *toc1* mutant
145 compared to that in *prp5*, *elf3*, or Col-0 plants (Fig. 1A-1D). This prompted us to compare the
146 expression patterns of *TOC1* and other *PRR* family members under SD and LD conditions.
147 Previously, it has been shown that the transcript and protein abundances of each *PRR* gene
148 peaks sequentially from dawn to dusk in the order of *PRR9*, *PRR7*, *PRR5*, *PRR3* and *TOC1*
149 (Matsushika et al., 2000; Fujiwara et al., 2008; Martin et al., 2018). However, whether the
150 distinct daylength information could change their mRNA or protein patterns remains unclear.
151 By using a time-course reverse transcription quantitative PCR (RT-qPCR) assay and the
152 publicly accessible database, we found that the expression pattern of *TOC1* was overall shifted
153 by about 4 h in SD vs. LD conditions, while the *PRR5* mRNA expression pattern was not
154 significantly altered by the daylength difference (Supplemental Fig. S3 and Supplemental Fig.

155 S4). Interestingly, when we compared the protein expression patterns of TOC1 and PRR5
156 between SD and LD conditions by using previously generated *TMG* (*TOC1* Mini Gene driven
157 by its native promoter) and *PRR5pro:PRR5-GFP* transgenic lines (Mas et al., 2003; Fujiwara
158 et al., 2008), we found that the duration and peak times of TOC1 and PRR5 proteins are highly
159 variable under these two distinct conditions. This might have been caused by
160 post-transcriptional regulation, given that the *PRR5* mRNA pattern did not display a phase
161 shift. Moreover, both PRR5 and TOC1 proteins were barely detectable at ZT20 in SD
162 conditions, but were still present in an appreciable level at ZT20 in LD conditions (Fig.
163 2A-2D). Remarkably, the high TOC1 protein level could even extend to ZT0 in the night under
164 LD conditions (Fig. 2A, 2B). In addition, the protein abundance of two other PRR family
165 members, PRR9 and PRR7, started to rise from ZT4, and persisted over the day time in both LD
166 and SD conditions. The PRR7 protein was maintained at a higher level with increasing
167 daylength (Fig. 2E-2H). Interestingly, among EC components, transcripts of *LUX* and *ELF4*
168 displayed a similar shifted pattern as *TOC1* in SD conditions, while *ELF3* only showed an
169 increased expression level without pattern shifting in SD conditions (Supplemental Fig.
170 S4E-4G). Thus, it appeared that the daylength information could either shift the expression
171 phase or extend the expression period of PRRs and EC at both the transcriptional and
172 post-transcriptional levels, which might contribute to the daylength-dependent photoperiodic
173 hypocotyl growth.

174 ***PIF4* and *PIF5* are Potential Common Transcriptional Targets of PRRs and EC**

175 To further elucidate the underlying mechanisms of how PRRs coordinate with EC to
176 regulate photoperiodic hypocotyl growth, we identified their direct transcriptional targets, as
177 both of them are transcription regulators (Gendron et al., 2012; Huang et al., 2012; Nakamichi
178 et al., 2012). RNA-sequencing (RNA-seq) with 10-day old seedlings of *toc1 prr5* grown under
179 12 h light/12 h dark conditions was conducted with tissues harvested at ZT15; the exact same
180 time point used for TOC1 ChIP-seq (Huang et al., 2012) and close to the time point for PRR5
181 ChIP-seq (Nakamichi et al., 2012). In total, we identified 838 differentially expressed genes
182 (DEGs) in the *toc1 prr5* double mutant using 2-fold cut-off (FDR<0.05) compared to Col-0

183 (Fig. 3A, Supplemental Dataset 1). The randomly selected 4 up-regulated genes and 4
184 down-regulated genes validated by RT-qPCR displayed similar expression patterns as that in
185 the RNA-seq data (Supplemental Fig. S5). Notably, *CIRCADIAN CLOCK ASSOCIATED 1*
186 (*CCA1*), *LATE ELONGATED HYPOCOTYL (LHY)*, and *GIGANTEA (GI)*, and some other
187 core circadian clock genes, were among the 270 up-regulated genes, consistent with the fact
188 that they are direct targets of TOC1 within the interlocked circadian clock oscillator (Huang et
189 al., 2012). Functional assignment of the DEGs by gene ontology (GO) enrichment analysis
190 further revealed that the DEGs were mainly involved in response to red or far-red light,
191 response to light stimulus, circadian rhythms, and red/far-red light photo-transduction (Fig.
192 3B), implicating a dual role for TOC1 and PRR5 in regulating the circadian clock and light
193 signaling. Among them, we found that transcript levels of *PIF4* and *PIF5* were significantly
194 increased in the *toc1 prr5* mutant (Fig. 3C). Previous ChIP-Seq analysis identified 772
195 TOC1-bound genes (Huang et al., 2012), 1021 PRR5-bound genes (Nakamichi et al., 2012),
196 and 1096 PRR7-bound genes (Liu et al., 2013). As the PRRs play redundant roles in regulating
197 photoperiodic hypocotyl growth, we thus compared the ChIP-seq data of PRR7, PRR5, and
198 TOC1, and obtained 90 commonly bound genes (Fig. 3D, Supplemental Fig. S6). The
199 interaction network analysis using the STRING database (<http://string-db.org/>) showed that the
200 90 common genes could form a major cluster, including known circadian clock genes, such as
201 *CCA1*, *LHY*, and *GI*, and genes involved in photomorphogenesis, including *PIF4*, *PIL6/PIF5*,
202 and *PHYTOCHROME B (PHYB)* (Fig. 3E). The potential direct target genes of PRRs were
203 further revealed by comparing our RNA-seq data with the PRR7/PRR5/TOC1 common target
204 genes. Strikingly, *PIF4* and *PIF5* were found among the 11 overlapping genes (Supplemental
205 Fig. S6, hypergeometric test, $p < 3.5 \times 10^{-9}$) between up-regulated genes in the *toc1 prr5* mutant
206 and the 90 common target genes, indicating that *PIF4* and *PIF5* were potential direct target
207 genes of TOC1 and PRR5. Furthermore, when we compared the aforementioned 11 overlapped
208 genes with the up-regulated genes in the *lux-6* mutant, *PIF4* and *PIF5* were again among the
209 only 4 common co-targets (Fig. 3F, 3G). Hence, *PIF4* and *PIF5* became promising target genes
210 of EC and PRRs in mediating their regulation of photoperiodic hypocotyl growth.

211 **PRRs directly Bind *PIF4* and *PIF5* Promoters to Repress Their Transcription**

212 As *PIF4* and *PIF5* are two potential common transcriptional targets of PRRs and EC, we
213 determined whether PRRs could directly repress *PIF4* and *PIF5* transcription. Promoter
214 analysis suggested that one potential TOC1 and PRR5 binding element, *PIF4-G* (G-box,
215 GATATG) (Gendron et al., 2012), was found at -707 bp upstream of the *PIF4* start codon, and
216 two G-boxes, *PIF5-G1* (G-box, GATATG) and *PIF5-G2* (G-box, GATATG), are found at
217 -1151 bp and -718 bp upstream of the *PIF5* start codon, respectively (Fig. 4A). We then
218 conducted electrophoretic mobility shift assays (EMSA) with the purified GST-tagged CCT
219 domain of TOC1 and PRR5, which is the DNA-binding domain of PRRs (Gendron et al., 2012).
220 Both GST-TOC1-CCT and GST-PRR5-CCT could efficiently bind the *PIF4-G* and *PIF5-G2*
221 regions compared to GST alone (Fig. 4B), as well as bind the *CCAI* promoter (as a positive
222 control) (Supplemental Fig S7A), but not the *PIF5-G1* region. Importantly, the binding could
223 be abolished by the non-labeled competitive probe, suggesting that TOC1 and PRR5 could
224 specifically bind the promoters of *PIF4* and *PIF5* (Fig. 4B and Supplemental Fig. S7A). Results
225 of ChIP-qPCR analysis further confirmed that the amplicons containing the *PIF4* promoter
226 G-box and *PIF5* promoter G2 regions were significantly enriched in *TMG* lines ranging from
227 ZT12 to ZT20 and in *PRR5:PRR5-GFP* from ZT8 to ZT16 (Fig. 4C, 4D), in line with the *TMG*
228 and PRR5 protein expression window. Similar binding enrichment was observed for the
229 amplicons for the *CCAI* promoter, but not the negative control *ASCORBATE PEROXIDASE 3*
230 (*APX3*) (Supplemental Fig. S7B, 7C). These results are consistent with previous ChIP-seq
231 studies (Huang et al., 2012, Nakamichi et al., 2012). Taken together, TOC1 and PRR5 could
232 directly bind *PIF4* and *PIF5* promoters *in vitro* and *in vivo*.

233 Whether TOC1 and PRR5 could directly repress *PIF4* and *PIF5* transcription was
234 determined by monitoring the bioluminescence signals of *PIF4pro:LUC* and *PIF5pro:LUC*
235 using well-established transient expression systems in the leaves of *Nicotiana benthamiana*
236 and in *Arabidopsis* protoplast. Results of the transient expression analyses clearly indicated that
237 the transcriptional activities of *PIF4* and *PIF5* could be repressed by PRRs (Fig. 4E-4H and

238 Supplemental Fig. S8). Collectively, our results supported the notion that *PIF4* and *PIF5* are
239 direct transcriptional targets of PRRs.

240 **PRRs Cooperate with EC in Timing Photoperiodic Transcription of *PIF4* and *PIF5***

241 As *PIF4* and *PIF5* are the common transcriptional targets of PRRs and EC, and daylength
242 could alter the expression patterns of PRRs and EC, we questioned whether PRR proteins could
243 coordinate with EC in conveying daylength information to control photoperiodic hypocotyl
244 growth through the timing of *PIF4* and *PIF5* transcription. To test this, *PIF5pro:PIF5-HA*
245 transgenic plants were generated to investigate the temporal protein pattern of PIF5 under SD
246 and LD conditions. Intriguingly, the PIF5 protein abundance was inversely associated with
247 TOC1 and PRR5 protein abundance (Fig. 2A-2D) under both SD (Fig. 5A) and LD (Fig. 5B)
248 conditions, consistent with the idea that TOC1 and PRR5 directly repressed *PIF5* transcription.
249 Similarly, PIF4 protein has been observed to accumulate during the light period and decrease in
250 the dark period from ZT12 to ZT20, then increase before dawn under a short day but not under
251 a 12 h light/12 h dark photoperiod. As PIF4 and PIF5 protein accumulation was associated well
252 with their transcription, *PIF4* and *PIF5* transcript levels were examined in the *toc1 prr5* double
253 mutant and *toc1 prr5 elf3* triple mutant. Results of RT-qPCR indicated that *PIF4* and *PIF5*
254 transcript levels were similar to that of Col-0 at the subjective day time in both *toc1 prr5* and
255 *toc1 prr5 elf3* mutants, but modestly increased at the subjective early night, and more
256 significantly accrued at late night, especially at ZT20 in both photoperiodic conditions (Fig.
257 5C-5F). As EC represses *PIF4* and *PIF5* transcription from dusk to early night, *PIF4* and *PIF5*
258 transcript levels displayed a modest but consistent increase in the *toc1 prr5 elf3* triple mutant
259 compared to those in *toc1 prr5* or *elf3* mutants, especially under LD conditions (Fig. 5C-5F).
260 Similarly, the transcript levels of *PIF4* and *PIF5* were also significantly elevated in *prp7 prp9*
261 and *prp5 prp7 prp9* mutants under both SD and LD conditions (Supplemental Fig. S9).
262 Together, our results support a notion that PRRs in concert with EC repress the transcription of
263 *PIF4* and *PIF5*, hence to shape their transcriptional patterns in mediating circadian
264 clock-regulated photoperiodic hypocotyl growth.

265 **Direct Transcriptional Inhibition of *PIF4* and *PIF5* by *TOC1* is Required for its**
266 **Regulation of Photoperiodic Hypocotyl Growth**

267 As the physical interaction of PRRs with PIFs antagonizes PIFs function under a diurnal
268 cycle (Martin et al., 2018; Soy et al., 2016; Zhu et al., 2016), a truncated *TOC1* without the
269 CCT DNA-binding domain (Gendron et al., 2012) was used to test if PRR-mediated *PIF4/5*
270 repression was required in photoperiodic hypocotyl growth. Similar to the full-length *TOC1*,
271 GFP-*TOC1*ΔCCT-NLS was predominantly localized in nuclear speckles both in the epidermal
272 cells of infiltrated *N. benthamiana* leaves and in the hypocotyl cells of stable transgenic
273 Arabidopsis plants (Supplemental Fig. S10). Importantly, the truncated *TOC1* protein without
274 its DNA binding domain could still physically interact with *PIF4* and *PIF5*, with a similar
275 affinity as full-length *TOC1* (Fig. 6A and Supplemental Fig. S11A), as the CCT domain was
276 dispensable in mediating *TOC1*-PIFs interaction in yeast (Zhu et al., 2016). However, the
277 transcriptional repression of *PIF4* and *PIF5* by the truncated *TOC1* protein without its CCT
278 domain was severely compromised compared to the full-length *TOC1* (Supplemental Fig. S12).
279 Notably, overexpression of full-length *TOC1*, but not *TOC1*ΔCCT, could fully rescue the long
280 hypocotyl phenotype of the *toc1-21* mutant grown in SD conditions, even when the *TOC1*
281 ectopic expression levels were comparable or lower than the endogenous *TOC1* (Fig. 6B).
282 Consistently, the transcript levels of *PIF4* and *PIF5* were significantly repressed by
283 overexpression of full-length *TOC1* but not *TOC1*ΔCCT (Fig. 6C). Compared to that in *toc1-21*
284 mutants, the moderately shortened hypocotyl phenotypes in the *TOC1*ΔCCT transgenic lines
285 was likely due to *TOC1*ΔCCT-PIFs interaction and sequestration of PIF function (Martin et al.,
286 2018; Soy et al., 2016; Zhu et al., 2016).

287 A missense allele of *toc1-1* caused by an A562V mutation in the *TOC1* DNA binding
288 domain (Strayer et al., 2000) was further employed to distinguish the direct transcriptional role
289 of *TOC1* on *PIF4* and *PIF5* from its post-translational regulation of PIFs via sequestration.
290 Similar to *TOC1*ΔCCT, the *TOC1* A562V protein could still physically interact with *PIF4* and
291 *PIF5* like the wild-type *TOC1* (Fig. 6D and Supplemental Fig. 11B). However, the *TOC1*
292 A562V had much reduced ability to bind *PIF4* and *PIF5* promoters in the EMSA (Fig. 6E),

293 similar to the results of a previous report on the binding of the *CCA1* promoter by TOC1 A562V
294 (Gendron et al., 2012). As the *toc1-1* mutant still displayed long hypocotyl phenotypes
295 (Dowson-Day and Millar, 1999) under SD conditions (Fig. 6F), it further supported the idea
296 that the TOC1-*PIFs* transcriptional module played a pivotal role in regulating photoperiodic
297 hypocotyl growth.

298 ***PIF4* and *PIF5* are Epistatic to *PRRs* in Regulating Photoperiodic Hypocotyl Growth**

299 As *PIF4* and *PIF5* are direct PRR transcriptional targets, together with the PRR physical
300 interaction with PIFs to sequester their activity (Martin et al., 2018; Soy et al., 2016; Zhu et al.,
301 2016), we proposed that *PIF4* and *PIF5* act as major downstream factors to mediate circadian
302 clock-regulated photoperiodic hypocotyl growth. Thus, we determined if *PIF4* and *PIF5* were
303 required for PRR-mediated circadian clock regulation of hypocotyl elongation by generating a
304 variety of higher order mutants. In agreement with a previous report (Soy et al., 2016), the long
305 hypocotyl phenotypes in *toc1* and *toc1 prr5* mutants could be partially reverted by a single
306 introgression of *pif4* under either LD or SD conditions. Moreover, the long hypocotyl
307 phenotype in the *toc1 prr5* mutant could be completely rescued to the wild-type (Col-0) level
308 by an introgression of *pif4 pif5* mutations under either LD or SD conditions (Fig. 7A-7D),
309 indicating a redundancy of *PIF4* and *PIF5* in mediating photoperiodic hypocotyl growth. The
310 hypocotyl length in various mutants including *toc1*, *toc1 pif4*, *pif4*, *toc1 prr5*, *pif4 pif5*, *toc1*
311 *prr5 pif4*, and *toc1 prr5 pif4 pif5*, were indistinguishable from that of Col-0 under continuous
312 light conditions (Fig. 7E-7F), further reinforcing the notion that the repression of *PIF4* and
313 *PIF5* by PRRs at both the transcriptional and post-transcriptional levels is required to
314 concurrently regulate photoperiodic hypocotyl growth by the circadian clock. Given a previous
315 report showing that mutations of *PIF4* and *PIF5* inhibit the long hypocotyls of *prr* mutants
316 (Martin et al., 2018; Soy et al., 2016) under SD conditions, our evidence further demonstrates
317 that *PIF4* and *PIF5* function downstream of PRRs to mediate photoperiodic hypocotyl growth.

318 **Discussion**

319 By sensing photoperiod, the plant circadian clock regulates a plethora of daily rhythmic
320 physiological events (Yanovsky and Kay, 2002; Valverde et al., 2004; Sanchez and Kay, 2016).
321 The hypocotyl displays a robust rhythmic elongation pattern under photoperiodic conditions by
322 a coincidental mechanism between the circadian clock and external light signals (Nozue et al.,
323 2007; Niwa et al., 2009; Nomoto et al., 2012). Nevertheless, how the circadian clock
324 coordinates with the external photoperiod to facilitate optimal hypocotyl growth remains
325 largely unknown. *PIF4* and *PIF5* have been characterized as potential targets of PRR5 and
326 PRR7 (Liu et al., 2013; Nakamichi et al., 2012). However, the temporal transcriptional
327 regulation of PRR proteins to *PIF4* and *PIF5*, especially under distinct photoperiodic cycles,
328 are still largely unclear. In this study, we found that PRRs genetically act additively with EC to
329 regulate photoperiodic hypocotyl growth. We further demonstrated that PRRs directly bound
330 the promoters of *PIF4* and *PIF5* to repress their transcription, and the altered temporal patterns
331 of PRRs by daylength information could subsequently change *PIF4* and *PIF5* mRNA
332 expression patterns, thus mediating photoperiodic hypocotyl growth (Fig. 8). By using specific
333 TOC1 alleles, our results unequivocally showed that the transcriptional regulation of *PIF4* and
334 *PIF5* is critical for PRR-regulated photoperiodic hypocotyl growth. In addition to
335 post-translational regulation of PIF abundance and activities by PRRs and ELF3 (Martin et al.,
336 2018; Nieto et al., 2015; Soy et al., 2016; Zhu et al., 2016), here we show that PRRs cooperate
337 with EC to control *PIF4* and *PIF5* temporal transcription patterns which mediates the crosstalk
338 between the circadian clock and light signaling to achieve optimal hypocotyl growth and fitness
339 under photoperiodic conditions.

340 Sensing and transmitting daylength information has long been proposed as an interplay
341 between the circadian clock and external photoperiod, with mainly unclear mechanisms.
342 Hypocotyls displays diel rhythmic growth patterns after emerging from the soil in natural
343 photoperiodic conditions, but the underlying molecular mechanism remains unclear.
344 Differential daylength information, i.e., a long day vs. short day, can drastically change the
345 expression pattern and period of *PRR* transcripts and proteins, indicating that daylength
346 information can be transmitted at least through PRRs and EC via both transcriptional and

347 post-transcriptional mechanisms. The altered expression pattern of PRRs, particularly for
348 TOC1 and PRR5, subsequently causes altered expression of *PIF4* and *PIF5* transcripts and
349 proteins, hence to affect daylength-dependent hypocotyl growth patterns (Fig. 5). The reason
350 why PRRs and EC act additively on the regulation of *PIF4* and *PIF5* transcription could be
351 explained by their differential binding sites within the *PIF4* and *PIF5* promoters, but not due to
352 the physical interaction between TOC1 and ELF3 (Huang et al., 2016). Hence, the biological
353 significance of TOC1 physically interacting with ELF3 awaits to be further explored.
354 Intriguingly, daylength information does not alter either the transcript level or expression
355 pattern of *PRR5* (Supplemental Fig. S3B), but the overall expression pattern of PRR5 protein
356 was shifted by about 4 h earlier in SD conditions (Fig. 2C, 2D), indicating that daylength
357 information sensing and transmission also occurs at the post-transcriptional level for
358 photoperiodic hypocotyl growth. A similar case has been observed for photoperiod-regulated
359 flowering time in which the CONSTANS (CO) protein level is tightly controlled by a
360 coincident mechanism between the circadian clock and photoperiod (Valverde et al., 2004;
361 Song et al., 2012). It will be of great interest to decipher how daylength information affects the
362 expression patterns of PRRs in future studies.

363 The expression of *PIF4* and *PIF5* oscillates with a peak after dawn, and then decreases
364 gradually (Nusinow et al., 2011). EC represses the expression of *PIF4* and *PIF5* at nighttime,
365 but aside from EC, how *PIF4* and *PIF5* are regulated by other circadian clock components at
366 the transcriptional level is still not clear. Our present findings here filled this knowledge gap,
367 and we proposed that, in LD conditions, the extended expression time-frame and the shifted
368 expression pattern together maximize the repression of PRRs on *PIF*s expression, thus
369 inhibiting hypocotyl growth. While in SD conditions, PRR5 and TOC1 proteins do not
370 accumulate before the subjective dawn range from ZT20 to ZT24, which causes high
371 abundance of *PIF4* and *PIF5* to promote hypocotyl growth. Taken together, our findings
372 revealed a key underlying mechanism by which the PRRs-*PIF4/5* transcriptional module finely
373 orchestrates circadian photoperiodic responsive hypocotyl growth in *Arabidopsis*.

374 Very recently, CCA1 and LHY, the two morning-phased circadian core components, were
375 shown to recruit SHORT HYPOCOTYL UNDER BLUE 1 (SHB1) to promote *PIF4*
376 transcription by directly binding to the *PIF4* promoter (Sun et al., 2019). Our EMSA results
377 (Fig. 3b, 5e and Supplemental Fig. 7) and previous evidence clearly demonstrated that PRRs
378 can bind the G-box cis-elements of *CCA1*, *PIF4*, and *PIF5* promoters to repress their
379 transcription. Collectively, the transcription of *PIF4* and *PIF5* was intricately modulated by the
380 circadian clock, among which CCA1 and LHY act as daytime transcriptional activators, while
381 PRRs and EC cooperatively act as transcription repressors to sequentially repress *PIF4* and
382 *PIF5* transcription (Fig. 6c). Meanwhile, PRRs and ELF3 also inhibit PIFs' activities at the
383 post-translational level by physically interacting with PIF proteins. Together, the complex
384 regulatory network, integrating both transcriptional and post-transcriptional regulation of PRRs
385 and EC on PIFs, collectively limits the function of PIFs from morning to early evening, to
386 precisely time the higher growth rate in the late night. Intriguingly, GI, another key circadian
387 clock protein, was recently reported to play a pivotal role in modulating light signaling through
388 physical interaction with PIFs (Nohales et al., 2019). GI protein not only negatively regulates
389 PIFs' protein stabilities, but also occupies PIFs' genomic target loci in the early evening
390 (Nohales et al., 2019). Hence, it is conceivable that the circadian clock tightly coordinates
391 photoperiodic hypocotyl growth by integrating multiple circadian regulation mechanisms on
392 PIFs at both the transcriptional and post-transcriptional levels. As *PIF4* and *PIF5* serve as a
393 central cellular signaling hub by integrating phytohormones, light signaling, and circadian
394 signals to control many downstream physiological processes, such as senescence (Song et al.,
395 2014; Nohales et al., 2019), shade avoidance and temperature signaling (Ma et al., 2016;
396 Pedmale et al., 2016), it will be of great interest in the future to investigate whether the
397 PRRs-*PIF4/5* transcriptional module plays other roles besides photoperiodic hypocotyl growth
398 control.

399 **Materials and Methods**

400 **Plant materials and growth conditions.** Except where indicated, all of the *Arabidopsis*
401 *thaliana* plants used in this study were in the Col-0 background, including WT, *toc1-21* (Ding

402 et al., 2007), *prp5-1* (Wang et al., 2010), *prp5-1 prp7-11* (Yamashino et al., 2008), *prp5-1*
403 *prp9-10* (Yamashino et al., 2008), *prp7-11 prp9-10* (Yamashino et al., 2008), *prp5-1 prp7-11*
404 *prp9-10* (Yamashino et al., 2008), *elf3-1* (Nusinow et al., 2011), *lux-6* (Zhang et al., 2018), *TMG*
405 (Mas et al., 2003), *PRR5pro:PRR5-GFP* (Fujiwara et al., 2008), *PRR7pro:PRR7-GFP*
406 (Fujiwara et al., 2008), *PRR9pro:PRR9-GFP* (Fujiwara et al., 2008), *pif4-2* (Leivar et al.,
407 2008), *pif4-2 pif5-3* (CS68096). *toc1-21 prp5-1*, *toc1-21 elf3-1*, *prp5-1 elf3-1*, *toc1-21 prp5-1*
408 *elf3-1*, *toc1-21 prp5-1 lux-6*, *toc1-21 pif4-2*, *toc1-21 prp5-1 pif4-2*, and *toc1-21 prp5-1 pif4-2*
409 *pif5-3* were generated by crossing. The sterilized Arabidopsis seeds were stratified at 4°C for 3
410 days, and then transferred to a 22°C growth chamber with light/dark cycles of 12 h light/12 h
411 dark, 16 h light/8 h dark, or 8 h light/16 h dark as indicated.

412

413 **Plasmids construction.** For the transient transcriptional repression assays in *Nicotiana*
414 *benthamiana*, the amplicons of *PIF4* and *PIF5* promoters from about 2000 base pairs upstream
415 of their start codons were amplified from Col-0 genomic DNA, then were inserted into the
416 promoter-free *pLUC-N-1300* vector between the *Pst* I and *Kpn* I sites to generate the
417 *PIF4pro:LUC-N-1300* and *PIF5pro:LUC-N-1300* constructs, respectively. To prepare the
418 vectors of *PIF4pro:LUC* and *PIF5pro:LUC* for Arabidopsis protoplast transient expression
419 analysis, the same sequences of *PIF4* and *PIF5* promoters were digested with *Bam*H I and
420 *Bsu*36 I, and then cloned into the *pLUC-999* vector.

421

422 **Hypocotyl length measurements.** Sterilized seeds were placed on MS medium (PhytoTech,
423 M524) for 3 days of incubation at 4°C, then incubated in specific light photoperiod conditions
424 (12 h light/12 h dark cycles, 16 h light/8 h dark, or 8 h light/16 h dark; white light: 200
425 $\mu\text{mol}\cdot\text{m}^{-2}\cdot\text{s}^{-1}$, Digital light meter, TES-1332A) for 5 additional days. Seedlings were
426 photographed and hypocotyl lengths were measured by using Image *J* software
427 (<http://rsb.info.nih.gov/ij>).

428

429 **Protein detection method for PRRs.** Seedlings of *TMG*, *PRR5pro:PRR5-GFP*,
430 *PRR7pro:PRR7-GFP* and *PRR9pro:PRR9-GFP* transgenic lines were grown under SD or LD
431 conditions (8 h light/16 h dark, or 16 h light/8 h dark; light intensity: $200\mu\text{mol}\cdot\text{m}^{-2}\cdot\text{s}^{-1}$, Digital
432 light meter, TES-1332A) for 10 days, and samples were harvested in 4-h intervals during a
433 24-hour cycle. Total proteins were extracted with IP buffer (50 mM Tris-Cl, pH 7.5, 150 mM
434 NaCl, 0.5% Nonidet P-40 (v/v), 1 mM EDTA, 1 mM dithiothreitol, 1 mM
435 phenylmethylsulfonyl fluoride, 5 $\mu\text{g}/\text{mL}$ leupeptin, 1 $\mu\text{g}/\text{mL}$ aprotinin, 1 $\mu\text{g}/\text{mL}$ pepstatin, 5
436 $\mu\text{g}/\text{mL}$ antipain, 5 $\mu\text{g}/\text{mL}$ chymostatin, 2 mM NaVO_3 , 2 mM NaF, 50 μM MG132, 50 μM
437 MG115, 50 μM ALLN). Supernatants were resolved using an 8% SDS-PAGE gel. The
438 respective proteins were detected by western blotting using GFP antibody (Abcam; ab6556).

439

440 **RNA-sequencing analysis.** For the RNA-seq assays, plants were grown under 12 h light / 12 h
441 dark conditions at 22°C for 10 days and harvested at ZT15. RNA-sequencing and differential
442 gene expression analyses were performed at Bionova (Beijing, China). In brief, RNA quality
443 was evaluated on a Bioanalyzer 2100 instrument (Agilent, Santa Clara, CA). Sequencing
444 libraries were prepared following the protocol of the Directional RNA Library Prep Kit (NEB
445 #E7760S). The 150 nt paired-end high-throughput sequencing was performed on an Illumina
446 HiSeq X TEN. Low quality sequencing reads were removed. Clean reads were mapped to the
447 Arabidopsis reference genome (TAIR10, www.arabidopsis.org) with Tophat2
448 (<https://ccb.jhu.edu/software/tophat/index.shtml>) software, and differentially expressed genes
449 (DEGs) were identified using edgeR in the R package

450 (<http://www.bioconductor.org/packages/release/bioc/html/edgeR.html>) with Fold Change > 2
451 and FDR < 0.05 between the case group sample and control group sample. Gene ontology (GO)
452 enrichment analysis was performed using TopGO in the R package (<http://bioconductor.org/>).

453

454 **Reverse Transcription Quantitative PCR for gene expression analysis.** Seedlings were
455 grown under specific light photoperiod conditions (12 h light/12 h dark, 16 h light/8 h dark, or 8
456 h light/16 h dark; light intensity: $200\mu\text{mol}\text{m}^2\text{s}^{-1}$) for 10 days, and samples were harvested in

457 4-h intervals during a 24-h period. Total RNA was extracted using TRIzol Reagent (Life
458 Technologies) as described by the manual. One microgram RNA was used for reverse
459 transcription with the PrimeScript RT Reagent Kit with gDNA Eraser (Takara). Quantitative
460 PCR was performed using SYBR Green Real-Time PCR Master Mix (Toyobo, Osaka, Japan)
461 according to the manufacturer's instructions on a QuantStudio 3 instrument (Applied
462 Biosystems, USA). The following PCR program was used: 95°C for 2 min, followed by 40
463 cycles of 95°C for 15 s, 55°C for 15 s, and 72°C for 15 s, followed by a melting-curve analysis.
464 Gene expression was normalized by the geometric mean of *ACTIN2* and *TUB4* expression as
465 previously described (Li et al., 2019). Experiments were repeated with at least two biological
466 and two technical replicates. Data represent means \pm SD of two technical replicates. Primers
467 used for quantitative PCR are listed in Supplemental Table 1.

468

469

470 **Transient transcriptional repression activity assay in *N. benthamiana*.** *Agrobacterium*
471 *tumefaciens* *AGL* carrying various fusion expression vectors (effector: *GFP-TOC1*,
472 *GFP-PRR5*, *GFP-PRR7*, *GFP-PRR9*, or *GFP*; reporter: *PIF4pro: LUC-1300*, *PIF5pro:*
473 *LUC-1300*, and *CCA1pro: LUC-1300*) were cultured overnight. Each reporter vector paired
474 with the *GFP-TOC1*, *GFP-PRR5*, *GFP-PRR7*, *GFP-PRR9*, or *GFP* effector vector was then
475 co-transformed into *N. benthamiana* leaves using a syringe infiltration method. The luciferase
476 signal was detected using a CCD camera (LN/1300-EB/1, Princeton Instruments) 2 days after
477 infiltration. The bioluminescence intensity of LUC signals was quantified by MetaMorph
478 Microscopy Automation and Image Analysis Software (Molecular Devices, San Jose, United
479 States).

480

481 **Arabidopsis protoplast transient expression analysis.** Protoplasts were isolated from rosette
482 leaves of four-week old Arabidopsis plants (Col-0). For transient expression assays, 200 μ L of
483 protoplast was transferred to a 2 mL microfuge tube containing 5 μ g effector plasmid, 3 μ g
484 reporter plasmid, and 2 μ g *35S::GUS* plasmid which was used as an internal control. The

485 effector:reporter:GUS were co-transformed into protoplasts at a ratio of 5:3:2., and the
486 LUC/GUS ratio was presented as normalized gene expression. *PIF4pro:LUC-1300*,
487 *PIF5pro:LUC-1300*, and *CCA1pro:LUC-1300* were used as reporters, and *35S:GFP-TOC1*,
488 *35S:GFP-PRR5*, *35S:GFP-PRR7*, *35S:GFP-PRR9*, and *35S: GFP* were used as effectors. The
489 protoplasts were incubated for 16–24 h at 22°C. The luminescence measurements were
490 acquired with a luciferase assay system (Promega, E1500) on a GloMax 20/20 luminometer
491 (Promega). The GUS activity was detected with 4-Methylumbelliferone glucuronide (MUG)
492 substrate (Alfa) on a GloMax 20/20 luminometer.

493 **Chromatin Immunoprecipitation (ChIP) assays.** ChIP assays were performed using *TMG*
494 and *PRR5pro:PRR5-GFP* transgenic lines grown under 22°C in a growth chamber with 12 h
495 light/12 h dark cycles for two weeks, and seedlings were harvested at 4-h intervals during a
496 24-h period (ZT0, ZT4, ZT8, ZT12, ZT16, and ZT20) as noted. ChIP experiments were
497 performed as described (Huang et al., 2012). GFP antibody (Invitrogen; ab11120) was used for
498 immunoprecipitation. The immunoprecipitates were analyzed by qPCR. Data are presented as
499 mean \pm SD, n = 3 from biological replicates. Primers used in this assay are shown in
500 Supplemental Table 1.

501
502 **Purified GST-tagged CCT domain of TOC1 and PRR5 proteins.** *GST-TOC1* or *PRR5-CCT*
503 plasmids were transformed into *Escherichia coli* BL21 strain, induced with 1 mM IPTG and
504 cultured overnight at 16°C. The cells were collected by centrifuging at 10,000 rpm for 10
505 minutes, then the cells were resuspended in 10 mL extraction buffer (50 mM Tris-Cl, pH 8.0,
506 250 mM NaCl, 5 mM EDTA, 1 mM phenylmethylsulfonyl fluoride, 5 μ g/mL leupeptin, 1
507 μ g/mL aprotinin, 1 μ g/mL pepstatin). Lysozyme was added and the reaction was incubated on
508 ice for 30 minutes, then 100 μ L 1M DTT and 1 mL 10% sarkosyl (w/v) were added and
509 thoroughly mixed. Then, the lysate was sonicated until it became transparent. 2.3 mL
510 Triton-X-100 was added and mixed for five minutes. After centrifuging at 10,000 rpm for 10
511 minutes, the supernatant was incubated with 500 μ L GST-resin at 4°C for 3 hours. The beads
512 were washed with wash buffer (50 mM Tris-Cl, pH 8.0, 150 mM NaCl, 1 mM EDTA, 3 mM

513 dithiothreitol, 1 mM phenylmethylsulfonyl fluoride, 0.5% Triton X-100 (v/v) for 5 times. The
514 GST-resin was eluted with a reduced glutathione solution to obtain a GST-TOC1 or
515 PRR5-CCT protein solution.

516

517 **EMSA.** The Lightshift Chemiluminescent EMSA kit (Thermo Scientific) was used for EMSA.
518 5 μ L GST-TOC1-CCT, GST-PRR5-CCT or GST protein and 0.5 μ L of each biotin-labeled
519 probe was used in all assays. Protein and probe were incubated in 1 \times Lightshift binding buffer,
520 0.05 μ g/ μ L poly(dI-dC), 2.5% (vol/vol) glycerol, 0.05% Nonidet P-40 (v/v), 50 mM KCl, and 5
521 mM MgCl₂ for 1 h at 4°C. Six percent gels were used. Gel running, transfer, and imaging were
522 done as described by the Lightshift kit as previously described (Gendron et al., 2012).

523

524 **Co-immunoprecipitation assay.** Agrobacteria containing *35S::TOC1-GFP* or *TOC1 CCT*
525 domain deletions, *35S::PRR5-GFP* or *PRR5 CCT* domain deletions, and *CsVMV::PIF4-HA* or
526 *CsVMV::PIF5-HA* were co-infiltrated into 4-week-old *N. benthamiana* leaves. The infiltrated
527 leaves were ground to a fine powder in liquid nitrogen after infiltration for 3 days. Total protein
528 was extracted with ice-cold IP buffer (50 mM Tris-Cl, pH 7.5, 150 mM NaCl, 0.5% Nonidet
529 P-40 (v/v), 1 mM EDTA, 1 mM dithiothreitol, 1 mM phenylmethylsulfonyl fluoride, 5 μ g/mL
530 leupeptin, 1 μ g/mL aprotinin, 1 μ g/mL pepstatin, 5 μ g/mL antipain, 5 μ g/mL chymostatin, 2
531 mM NaVO₃, 2 mM NaF, 50 μ M MG132, 50 μ M MG115, 50 μ M ALLN). The cleared
532 supernatant was incubated with Protein A beads (Invitrogen, Cat no. 15918-014) with captured
533 anti-GFP (Invitrogen; ab11120) antibody at 4°C for 2 h. The immune complex was released
534 from the resin by 6 \times SDS loading buffer. Supernatants were resolved using an 8% SDS-PAGE
535 gel. GFP-tagged TOC1 and PRR5 and HA-tagged PIF4 and PIF5 were detected by western
536 blotting using GFP antibody (Abcam; ab6556) and HA antibody (Roche; 3F10), respectively.

537

538 **Statistical analysis.** Differences between means were statistically analyzed by one-way
539 analysis of variance using Tukey's *b post hoc* multiple comparison test (IBM SPSS Statistics
540 Software) or Student's *t*-test (Excel, Microsoft) as indicated in the figure legends. Statistically

541 significant differences were defined as those with p values < 0.05 . Significance levels are
542 indicated as * $p < 0.05$, ** $p < 0.01$, and *** $p < 0.001$.

543

544 **Accession numbers**

545 The Arabidopsis Genome Initiative numbers for the genes mentioned in this article are as
546 follows: *TOC1*, *AT5G61380*; *PRR5*, *AT5G24470*; *PRR7*, *AT5G02810*; *PRR9*, *AT2G46790*;
547 *PIF4*, *AT2G43010*; *PIF5*, *AT3G59060*; *YUC8*, *AT4G28720*; *IAA19*, *AT3G15540*; *ATHB2*,
548 *AT4G16780*; *ELF3*, *AT2G25930*; *ELF4*, *AT2G40080*; *LUX*, *AT3G46640*. RNA-seq data
549 reported in this study have been deposited in the Gene Expression Omnibus database under
550 accession number GSE99290.

551

552 **Supplemental Data**

553 **Supplemental Figure S1.** *TOC1* and *PRR5* regulate photoperiodic hypocotyl growth
554 independent of *LUX*.

555 **Supplemental Figure S2.** The hypocotyl phenotypes of *prrr57*, *prrr59*, *prrr79*, and *prrr579*
556 mutants in different photoperiod conditions.

557 **Supplemental Figure S3.** Time-course expression pattern of *TOC1/PRR5* in short-day or
558 long-day conditions.

559 **Supplemental Figure S4.** Time-course expression pattern of *PRRs* and *EC* components in
560 short-day or long-day conditions.

561 **Supplemental Figure S5.** Validation of RNA-seq results by reverse transcription quantitative
562 PCR.

563 **Supplemental Figure S6.** *PIF4* and *PIF5* were found among the 11 overlapping genes
564 between up-regulated genes in the *toc1 prr5* mutant and co-bound genes by *TOC1*, *PRR5*, and
565 *PRR7*.

566 **Supplemental Figure S7.** *TOC1* and *PRR5* bind the *CCA1* promoter but not the *APX3*
567 promoter.

568 **Supplemental Figure S8.** PRR7 and PRR9 directly repress *PIF4* and *PIF5* transcription.
569 **Supplemental Figure S9.** The transcriptional pattern of *PIF4* and *PIF5* in *prp* mutants under
570 different photoperiod conditions.
571 **Supplemental Figure S10.** Subcellular localization of GFP-TOC1 and
572 GFP-TOC1 Δ CCT-NLS proteins.
573 **Supplemental Figure S11.** Physical interactions between TOC1, TOC1 Δ CCT, TOC1-A562V,
574 and PIF5.
575 **Supplemental Figure S12.** The transcriptional inhibition of *PIF4* and *PIF5* by TOC1 Δ CCT
576 was significantly attenuated.
577 **Supplemental Table S1.** Primers used in this study.
578 **Supplemental Dataset S1.** The differentially expressed genes (DEGs) in the *toc1 prr5* double
579 mutant identified by RNA-seq.

580

581 **Acknowledgements**

582 We are grateful to Profs. JC Jang and David E. Somers for their constructive and critical
583 comments on this manuscript, and thank Ms. Jingquan Li from the Key Laboratory of Plant
584 Molecular Physiology and Plant Science Facility of the Institute of Botany, Chinese Academy
585 of Sciences for her excellent technical assistance with confocal microscopy.

586

587 **Figure legends**

588 **Figure 1.** TOC1 and PRR5 coordinate with EC to regulate photoperiodic hypocotyl growth. A,
589 Hypocotyl phenotypes of Col-0, *toc1*, *elf3*, *toc1 elf3*, *prr5*, *prr5 elf3*, *toc1 prr5*, and *toc1 prr5*
590 *elf3* seedlings grown under short-day conditions (8L/16D) for 5 days after germination as
591 noted. Scale bar, 5 mm. B, Quantitative analysis of the hypocotyl length of the seedlings shown
592 in A. Different letters indicate statistically significant differences among averages by Tukey's b
593 test ($p < 0.05$). Data are the means \pm SD of more than 15 seedlings. C, Hypocotyl phenotypes of
594 Col-0, *toc1*, *elf3*, *toc1 elf3*, *prr5*, *prr5 elf3*, *toc1 prr5*, and *toc1 prr5 elf3* seedlings grown under

595 long-day conditions (16L/8D) for 5 days after germination as noted. Scale bar, 5 mm. D,
596 Quantitative analysis of the hypocotyl length of the seedlings shown in (C). Different letters
597 indicate statistically significant differences among averages by Tukey's b test ($p < 0.05$). Data
598 are the means \pm SD of more than 15 seedlings. E, Hypocotyl phenotypes of Col-0, *toc1*, *elf3*,
599 *toc1 elf3*, *prr5*, *prr5 elf3*, *toc1 prr5*, and *toc1 prr5 elf3* seedlings grown under continuous white
600 light conditions for 5 days after germination as noted. Scale bar, 5 mm. Seedling images in A, C
601 and E were digitally abstracted and multiple images were made into a composite for
602 comparison. F, Quantitative analysis of the hypocotyl length of the seedlings shown in (E).
603 Different letters indicate statistically significant differences among averages by Tukey's b test
604 ($p < 0.05$). Data are the means \pm SD of more than 15 seedlings.

605

606 **Figure 2.** PRR protein expression patterns in differential photoperiod conditions.

607 A to H, Immunoblots showing TOC1/PRR5/ PRR7/ PRR9 protein abundance in seedlings of
608 *TMG*, *PRR5pro:PRR5-GFP*, *PRR7pro:PRR7-GFP* and *PRR9pro:PRR9-GFP*, respectively,
609 grown in short day or long day conditions for 10 days. Coomassie Brilliant Blue (CBB) staining
610 indicates the protein loading amount. Data are representative of three biological replicates with
611 similar results.

612 **Figure 3.** *PIF4* and *PIF5* are potential direct transcriptional targets of TOC1 and PRR5. A,
613 Differentially expressed genes (DEGs) between the *toc1 prr5* mutant and wild-type Col-0 in
614 RNA-seq. The samples were harvested at ZT15 from 10-day-old seedlings grown in 12 h
615 light/12 h dark photoperiods. B, Gene ontology (GO) analysis of the overlapping genes between
616 upregulated DEGs in the *toc1 prr5* mutant and the bound genes by TOC1. C, Expression
617 profiles of *PIF4* and *PIF5* in the *toc1 prr5* mutant. Data from RNA-seq. D, Venn diagram
618 showing the number of common genes bound by TOC1, PRR5, and PRR7. E, Protein
619 interaction network analysis of the 90 co-bound genes by TOC1, PRR5, and PRR7 in (D) using
620 the STRING database (<http://string-db.org/>), showing a major cluster including *PIF4*, *PIF5*,
621 and other known circadian core components. Colored nodes: query proteins and first shell of
622 interactors; white nodes: second shell of interactors; empty nodes: proteins of unknown 3D

623 structure; filled nodes: some 3D structure is known or predicted. Edges represent
624 protein-protein associations; light blue edges: from curated databases; purple edges:
625 experimentally determined; green edges: gene neighborhood; dark blue: gene co-occurrence;
626 yellow edges: text mining; dark edges: co-expression; light purple edges: protein homology. F,
627 Venn diagram showing the number of overlapping genes among the TOC1, PRR5, and PRR7
628 co-bound genes, upregulated DEGs in the *toc1 prr5* mutant, and upregulated DEGs in the *lux-6*
629 mutant. G, Heatmap showing 4 common co-targets in upregulated DEGs in *toc1 prr5* and *lux-6*
630 mutants. Scale represents \log_2 (fold change).

631 **Figure 4.** TOC1 and PRR5 directly bind the *PIF4* and *PIF5* promoters to repress their
632 transcription. A, Schematic diagram of the promoter regions of *PIF4* and *PIF5*. Orange boxes
633 represent the putative G-box elements. G, G1, and G2 represent the respective DNA fragments
634 used for generating EMSA probes and ChIP-qPCR detection. B, EMSA with the CCT domain
635 of TOC1 and PRR5 incubated with a probe designed for the *PIF4-G*, *PIF5-G1*, and *PIF5-G2*
636 regions of the *PIF5* gene as shown in (A), and 100-fold unlabeled competitor (100 \times). GST
637 alone was used as a negative control. Arrowheads mark the shifted bands. C and D,
638 Time-course ChIP-qPCR assay showing that TOC1 and PRR5 bind to the *PIF4-G* (C) and
639 *PIF5-G2* (D) regions diurnally, which was well associated with their respective protein
640 abundances. Data are the means \pm SD. E, Transient transcriptional expression analysis
641 showing that *PIF4* and *PIF5* were repressed by TOC1 and PRR5 in epidermal cells of *N.*
642 *benthamiana* leaves. *CCA1pro:LUC* was used as a positive control. Data are representative of
643 three biological replicates with similar results. Leaf images were digitally abstracted and
644 multiple images were made into a composite for comparison. F, Quantification of
645 bioluminescence intensity as shown in (E). Data are the means \pm SD. The asterisks denote
646 statistically significant differences among means, * $p < 0.05$, ** $p < 0.01$, *** $p < 0.001$ by
647 Student's *t*-test. G and H, Transient transcriptional expression assay in Arabidopsis protoplasts.
648 A schematic diagram of effector and reporter vectors is shown in (G). Respective quantification
649 of relative LUC/GUS activity is shown in (H). The relative LUC/GUS activity in protoplasts
650 co-transformed with GFP and reporter vector was defined as 1. *CCA1pro:LUC* was used as a

651 positive control, while 35S:*GUS* was used as an internal control. Data are the means \pm SD. The
652 asterisks in (H) denote statistically significant differences among means, * $p < 0.05$, ** $p < 0.01$,
653 *** $p < 0.001$ by Student's *t*-test .

654 **Figure 5.** TOC1 and PRR5 coordinate with EC to transmit daylength information for shaping
655 *PIF4* and *PIF5* transcription. A and B, Immunodetection of PIF5 protein levels in
656 *PIF5pro:PIF5-HA* transgenic seedlings. Extracts from seedlings grown in short day (A) and
657 long day (B) conditions for 10 days. CBB staining indicates the protein loading. Data are
658 representative of three biological replicates with similar results. C and D, RT-qPCR analysis
659 showing *PIF5* transcript levels in Col-0, *toc1 prr5*, *elf3*, and *toc1 prr5 elf3* seedlings grown for
660 10 days in short day (C) or long day (D) conditions. E and F, RT-qPCR analysis showing *PIF4*
661 transcript levels in Col-0, *toc1 prr5*, *elf3*, and *toc1 prr5 elf3* seedlings grown for 10 days in
662 short day (E) and long day (F) conditions. From (C) to (F), data are the means \pm SD., white and
663 black rectangles below the graphs represent day and night respectively.

664 **Figure 6.** Direct transcriptional inhibition of *PIF4* and *PIF5* by TOC1 is required for its
665 regulation of photoperiodic hypocotyl growth. A, Physical interactions between TOC1,
666 TOC1 Δ CCT (1-532aa)-NLS, and *PIF4* *in vivo* were detected by co-immunoprecipitation after
667 transient co-expression in *N. benthamiana*. B Hypocotyl phenotypes of *toc1-21*, *GFP-TOC1*/
668 *toc1-21*, and *GFP-TOC1 Δ CCT-NLS* / *toc1-21* transgenic seedlings grown under short day
669 conditions (8L/16D) for 5 days after germination. Seedling images were digitally abstracted
670 and multiple images were made into a composite for comparison. The protein levels of
671 GFP-TOC1 and GFP-TOC1 Δ CCT-NLS in these transgenic seedlings were also detected by
672 immunoblot. Representative seedlings were photographed as shown in the left panel, and the
673 hypocotyl lengths of the seedlings shown in the left panel were quantified and are shown in the
674 right panel. Scale bar, 5 mm. Data are the means \pm SD of more than 20 seedlings. Different
675 letters indicate statistically significant differences among averages by Tukey's b test ($p < 0.05$).
676 C, RT-qPCR analysis of *PIF4* and *PIF5* expression in *toc1-21*, *GFP-TOC1 toc1-21*, and
677 *GFP-TOC1 Δ CCT-NLS toc1-21* transgenic seedlings grown for 10 days in short day conditions

678 at ZT12. Data are the means \pm SD. The asterisks denote statistically significant differences
679 among means, * $p < 0.05$, ** $p < 0.01$, *** $p < 0.001$ by Student's t -test. D, Physical interaction
680 between TOC1-A562V and PIF4 was detected by co-immunoprecipitation after being
681 transiently co-expressed in leaves of *N. benthamiana*. The immunoprecipitates with human IgG
682 beads were analyzed by immunoblot with anti-PAP or anti-HA antibody as indicated. E, EMSA
683 with CCT and CCT-A562V of TOC1 and GST incubated with a probe designed to the *PIF4-G*
684 and *PIF5-G2* regions, and 100-fold unlabeled competitor (100 \times). Arrowheads mark the shifted
685 bands. F, Hypocotyl phenotypes of wild type (C24 ecotype) and *toc1-1* grown for 5 days in
686 short day conditions. Representative seedlings were photographed (left panel) and measured
687 (right panel). Data are the means \pm SD of more than 20 seedlings. The asterisks denote
688 statistically significant differences among means, *** $p < 0.001$ by Student's t -test.

689
690 **Figure 7.** *PIF4* and *PIF5* are epistatic to *TOC1* and *PRR5* for photoperiodic hypocotyl growth.
691 A and B, Hypocotyl phenotypes of Col-0, *toc1*, *pif4*, *toc1 pif4*, *toc1 prr5*, *toc1 prr5 pif4*, *pif4*
692 *pif5*, and *toc1 prr5 pif4 pif5* seedlings (5 DAG) grown under short day conditions (8L/16D). C
693 and D, Hypocotyl phenotypes of Col-0, *toc1*, *pif4*, *toc1 pif4*, *toc1 prr5*, *toc1 prr5 pif4*, *pif4 pif5*,
694 and *toc1 prr5 pif4 pif5* seedlings (5 DAG) grown under long day conditions (16L/8D). E and F,
695 Hypocotyl phenotypes of Col-0, *toc1*, *pif4*, *toc1 pif4*, *toc1 prr5*, *toc1 prr5 pif4*, *pif4 pif5*, and
696 *toc1 prr5 pif4 pif5* seedlings (5 DAG) grown under continuous white light conditions.
697 Representative seedlings were photographed as shown in (A), (C) and (E). Seedling images
698 were digitally abstracted and multiple images were made into a composite for comparison.
699 Scale bar, 5 mm. Hypocotyl lengths of the seedlings were measured and quantified as shown in
700 (B), (D) and (F). Different letters indicate statistically significant differences among means by
701 Tukey's b test ($p < 0.05$). Data are the means \pm SD of more than 15 seedlings.

702 **Figure 8.** A proposed working model for PRR-*PIF4/5* transcriptional module-mediated
703 photoperiodic hypocotyl growth. PSEUDO RESPONSE REGULATORS (PRRs), as core
704 circadian clock components, can directly and sequentially bind the promoters of

705 *PHYTOCHROME INTERACTING FACTOR 4 (PIF4)* and *PIF5* to repress their transcription
706 in an independent manner with Evening Complex. Diurnal rhythms of PIF4/5 protein
707 abundance are determined by the coordination of light signaling-mediated protein stability and
708 circadian clock-regulated transcriptional expression. Hence, TOC1 and other PRRs represent a
709 primary molecular node between the circadian clock and photoperiod to control photoperiodic
710 hypocotyl growth.

711

712 REFERENCES

- 713 **Al-Sady B, Ni W, Kircher S, Schafer E, Quail PH (2006)** Photoactivated phytochrome
714 induces rapid PIF3 phosphorylation prior to proteasome-mediated degradation. *Mol Cell*
715 **23**: 439-446
- 716 **Andres F, Coupland G (2012)** The genetic basis of flowering responses to seasonal cues. *Nat*
717 *Rev Genet* **13**: 627-639
- 718 **Dowson-Day MJ, Millar AJ (1999)** Circadian dysfunction causes aberrant hypocotyl
719 elongation patterns in *Arabidopsis*. *Plant J* **17**: 63-71
- 720 **Ding Z, Doyle MR, Amasino RM, Davis SJ (2007)** A complex genetic interaction between
721 *Arabidopsis thaliana* TOC1 and CCA1/LHY in driving the circadian clock and in output
722 regulation. *Genetics* **176**: 1501-1510
- 723 **Fujimori T, Yamashino T, Kato T, Mizuno T (2004)** Circadian-controlled
724 basic/helix-loop-helix factor, PIL6, implicated in light-signal transduction in *Arabidopsis*
725 *thaliana*. *Plant Cell Physiol* **45**: 1078-1086
- 726 **Fujiwara S, Wang L, Han L, Suh SS, Salome PA, McClung CR, Somers DE (2008)**
727 Post-translational regulation of the *Arabidopsis* circadian clock through selective
728 proteolysis and phosphorylation of pseudo-response regulator proteins. *J Biol Chem* **283**:
729 23073-23083

730 **Gendron JM, Pruneda-Paz JL, Doherty CJ, Gross AM, Kang SE, Kay SA (2012)**
731 *Arabidopsis* circadian clock protein, TOC1, is a DNA-binding transcription factor. Proc
732 Natl Acad Sci USA **109**: 3167-3172

733 **Hazen SP, Schultz TF, Pruneda-Paz JL, Borevitz JO, Ecker JR, Kay SA (2005) LUX**
734 ARRHYTHMO encodes a Myb domain protein essential for circadian rhythms. Proc Natl
735 Acad Sci USA **102**: 10387-10392

736 **Huang H, Alvarez S, Bindbeutel R, Shen Z, Naldrett MJ, Evans BS, Briggs SP, Hicks**
737 **LM, Kay SA, Nusinow DA (2016) Identification of Evening Complex Associated**
738 **Proteins in *Arabidopsis* by Affinity Purification and Mass Spectrometry. Mol Cell**
739 **Proteomics **15**: 201-217**

740 **Huang W, Perez-Garcia P, Pokhilko A, Millar AJ, Antoshechkin I, Riechmann JL, Mas P**
741 **(2012) Mapping the core of the *Arabidopsis* circadian clock defines the network structure**
742 **of the oscillator. Science **336**: 75-79**

743 **Huq E, Quail PH (2002) PIF4, a phytochrome-interacting bHLH factor, functions as a**
744 **negative regulator of phytochrome B signaling in *Arabidopsis*. EMBO J **21**: 2441-2450**

745 **Kaczorowski KA, Quail PH (2003) *Arabidopsis* PSEUDO-RESPONSE REGULATOR7 is a**
746 **signaling intermediate in phytochrome-regulated seedling deetiolation and phasing of the**
747 **circadian clock. Plant Cell **15**: 2654-2665**

748 **Lee BD, Kim MR, Kang MY, Cha JY, Han SH, Nawkar GM, Sakuraba Y, Lee SY,**
749 **Imaizumi T, McClung CR, Kim WY, Paek NC (2017) The F-box protein FKF1 inhibits**
750 **dimerization of COP1 in the control of photoperiodic flowering. Nat Commun **8**: 2259**

751 **Leivar P, Monte E, Al-Sady B, Carle C, Storer A, Alonso JM, Ecker JR, Quail PH (2008)**
752 **The *Arabidopsis* phytochrome-interacting factor PIF7, together with PIF3 and PIF4,**
753 **regulates responses to prolonged red light by modulating phyB levels. Plant Cell **20**:**
754 **337-352**

755 **Li B, Wang Y, Zhang Y, Tian W, Chong K, Jang JC, and Wang L (2019) PRR5, 7 and 9 positively**
756 **modulate TOR signaling-mediated root cell proliferation by repressing TANDEM ZINC**
757 **FINGER 1 in *Arabidopsis*. Nucleic Acids Res **47**:5001-5015.**

-
- 758 **Liu T, Carlsson J, Takeuchi T, Newton L, Farre EM** (2013) Direct regulation of abiotic
759 responses by the *Arabidopsis* circadian clock component PRR7. *Plant J* **76**: 101-114
- 760 **Liu TL, Newton L, Liu MJ, Shiu SH, Farre EM** (2016) A G-Box-Like Motif Is Necessary
761 for Transcriptional Regulation by Circadian Pseudo-Response Regulators in *Arabidopsis*.
762 *Plant Physiol* **170**: 528-539
- 763 **Ma D, Li X, Guo Y, Chu J, Fang S, Yan C, Noel JP, Liu H** (2016) Cryptochrome 1 interacts
764 with PIF4 to regulate high temperature-mediated hypocotyl elongation in response to blue
765 light. *Proc Natl Acad Sci USA* **113**: 224-229
- 766 **Martin G, Rovira A, Veciana N, Soy J, Toledo-Ortiz G, Gommers CMM, Boix M,**
767 **Henriques R, Minguet EG, Alabadi D, Halliday KJ, Leivar P, Monte E** (2018)
768 Circadian Waves of Transcriptional Repression Shape PIF-Regulated
769 Photoperiod-Responsive Growth in *Arabidopsis*. *Curr Biol* **28**: 311-318 e315
- 770 **Mas P, Kim WY, Somers DE, Kay SA** (2003) Targeted degradation of TOC1 by ZTL
771 modulates circadian function in *Arabidopsis thaliana*. *Nature* **426**: 567-570
- 772 **Matsushika A, Makino S, Kojima M, Mizuno T** (2000) Circadian waves of expression of the
773 APRR1/TOC1 family of pseudo-response regulators in *Arabidopsis thaliana*: insight into
774 the plant circadian clock. *Plant Cell Physiol* **41**: 1002-1012
- 775 **Millar AJ** (2016) The Intracellular Dynamics of Circadian Clocks Reach for the Light of
776 Ecology and Evolution. *Annu Rev Plant Biol* **67**: 595-618
- 777 **Nakamichi N, Kiba T, Henriques R, Mizuno T, Chua NH, Sakakibara H** (2010)
778 PSEUDO-RESPONSE REGULATORS 9, 7, and 5 are transcriptional repressors in the
779 *Arabidopsis* circadian clock. *Plant Cell* **22**: 594-605
- 780 **Nakamichi N, Kiba T, Kamioka M, Suzuki T, Yamashino T, Higashiyama T, Sakakibara**
781 **H, Mizuno T** (2012) Transcriptional repressor PRR5 directly regulates clock-output
782 pathways. *Proc Natl Acad Sci USA* **109**: 17123-17128
- 783 **Nakamichi N, Kita M, Ito S, Yamashino T, Mizuno T** (2005) PSEUDO-RESPONSE
784 REGULATORS, PRR9, PRR7 and PRR5, together play essential roles close to the
785 circadian clock of *Arabidopsis thaliana*. *Plant Cell Physiol* **46**: 686-698

786 **Nieto C, Lopez-Salmeron V, Daviere JM, Prat S** (2015) ELF3-PIF4 interaction regulates
787 plant growth independently of the Evening Complex. *Curr Biol* **25**: 187-193

788 **Niwa Y, Yamashino T, Mizuno T** (2009) The circadian clock regulates the photoperiodic
789 response of hypocotyl elongation through a coincidence mechanism in *Arabidopsis*
790 *thaliana*. *Plant Cell Physiol* **50**: 838-854

791 **Nohales MA, Liu W, Duffy T, Nozue K, Sawa M, Pruneda-Paz JL, Maloof JN, Jacobsen**
792 **SE, Kay SA** (2019) Multi-level Modulation of Light Signaling by GIGANTEA Regulates
793 Both the Output and Pace of the Circadian Clock. *Dev Cell* **49**: 840-851 e848

794 **Nomoto Y, Kubozono S, Miyachi M, Yamashino T, Nakamichi N, Mizuno T** (2012) A
795 circadian clock- and PIF4-mediated double coincidence mechanism is implicated in the
796 thermosensitive photoperiodic control of plant architectures in *Arabidopsis thaliana*. *Plant*
797 *Cell Physiol* **53**: 1965-1973

798 **Nozue K, Covington MF, Duek PD, Lorrain S, Fankhauser C, Harmer SL, Maloof JN**
799 (2007) Rhythmic growth explained by coincidence between internal and external cues.
800 *Nature* **448**: 358-361

801 **Nusinow DA, Helfer A, Hamilton EE, King JJ, Imaizumi T, Schultz TF, Farre EM, Kay**
802 **SA** (2011) The ELF4-ELF3-LUX complex links the circadian clock to diurnal control of
803 hypocotyl growth. *Nature* **475**: 398-402

804 **Pedmale UV, Huang SC, Zander M, Cole BJ, Hetzel J, Ljung K, Reis PAB, Sridevi P,**
805 **Nito K, Nery JR, Ecker JR, Chory J** (2016) Cryptochromes Interact Directly with PIFs
806 to Control Plant Growth in Limiting Blue Light. *Cell* **164**: 233-245

807 **Quint M, Delker C, Franklin KA, Wigge PA, Halliday KJ, van Zanten M** (2016)
808 Molecular and genetic control of plant thermomorphogenesis. *Nat Plants* **2**: 15190

809 **Sakuraba Y, Jeong J, Kang MY, Kim J, Paek NC, Choi G** (2014) Phytochrome-interacting
810 transcription factors PIF4 and PIF5 induce leaf senescence in *Arabidopsis*. *Nat Commun*
811 **5**: 4636

812 **Sanchez SE, Kay SA** (2016) The Plant Circadian Clock: From a Simple Timekeeper to a
813 Complex Developmental Manager. *Cold Spring Harb Perspect Biol* **8**: a027748

814 **Sato E, Nakamichi N, Yamashino T, Mizuno T** (2002) Aberrant expression of the
815 *Arabidopsis* circadian-regulated APRR5 gene belonging to the APRR1/TOC1 quintet
816 results in early flowering and hypersensitiveness to light in early photomorphogenesis.
817 *Plant Cell Physiol* **43**: 1374-1385

818 **Sawa M, Kay SA** (2011) GIGANTEA directly activates Flowering Locus T in *Arabidopsis*
819 *thaliana*. *Proc Natl Acad Sci USA* **108**: 11698-11703

820 **Sawa M, Nusinow DA, Kay SA, Imaizumi T** (2007) FKF1 and GIGANTEA complex
821 formation is required for day-length measurement in *Arabidopsis*. *Science* **318**: 261-265

822 **Shen Y, Khanna R, Carle CM, Quail PH** (2007) Phytochrome induces rapid PIF5
823 phosphorylation and degradation in response to red-light activation. *Plant Physiol* **145**:
824 1043-1051

825 **Song Y, Yang C, Gao S, Zhang W, Li L, Kuai B** (2014) Age-triggered and dark-induced leaf
826 senescence require the bHLH transcription factors PIF3, 4, and 5. *Mol Plant* **7**: 1776-1787

827 **Song YH, Smith RW, To BJ, Millar AJ, Imaizumi T** (2012) FKF1 conveys timing
828 information for CONSTANS stabilization in photoperiodic flowering. *Science* **336**:
829 1045-1049

830 **Soy J, Leivar P, Gonzalez-Schain N, Martin G, Diaz C, Sentandreu M, Al-Sady B, Quail**
831 **PH, Monte E** (2016) Molecular convergence of clock and photosensory pathways
832 through PIF3-TOC1 interaction and co-occupancy of target promoters. *Proc Natl Acad Sci*
833 *USA* **113**: 4870-4875

834 **Strayer C, Oyama T, Schultz TF, Raman R, Somers DE, Mas P, Panda S, Kreps JA, Kay**
835 **SA** (2000) Cloning of the *Arabidopsis* clock gene TOC1, an autoregulatory response
836 regulator homolog. *Science* **289**: 768-771

837 **Sun Q, Wang S, Xu G, Kang X, Zhang M, Ni M** (2019) SHB1 and CCA1 interaction
838 desensitizes light responses and enhances thermomorphogenesis. *Nat Commun* **10**: 3110

839 **Valverde F, Mouradov A, Soppe W, Ravenscroft D, Samach A, Coupland G** (2004)
840 Photoreceptor regulation of CONSTANS protein in photoperiodic flowering. *Science*
841 **303**: 1003-1006

842 **Wang L, Fujiwara S, Somers DE** (2010) PRR5 regulates phosphorylation, nuclear import and
843 subnuclear localization of TOC1 in the *Arabidopsis* circadian clock. *EMBO J* **29**:
844 1903-1915

845 **Yamamoto Y, Sato E, Shimizu T, Nakamich N, Sato S, Kato T, Tabata S, Nagatani A,**
846 **Yamashino T, Mizuno T** (2003) Comparative genetic studies on the APRR5 and APRR7
847 genes belonging to the APRR1/TOC1 quintet implicated in circadian rhythm, control of
848 flowering time, and early photomorphogenesis. *Plant Cell Physiol* **44**: 1119-1130

849 **Yamashino T, Ito S, Niwa Y, Kunihiro A, Nakamichi N, Mizuno T** (2008) Involvement of
850 *Arabidopsis* clock-associated pseudo-response regulators in diurnal oscillations of gene
851 expression in the presence of environmental time cues. *Plant Cell Physiol* **49**: 1839-1850

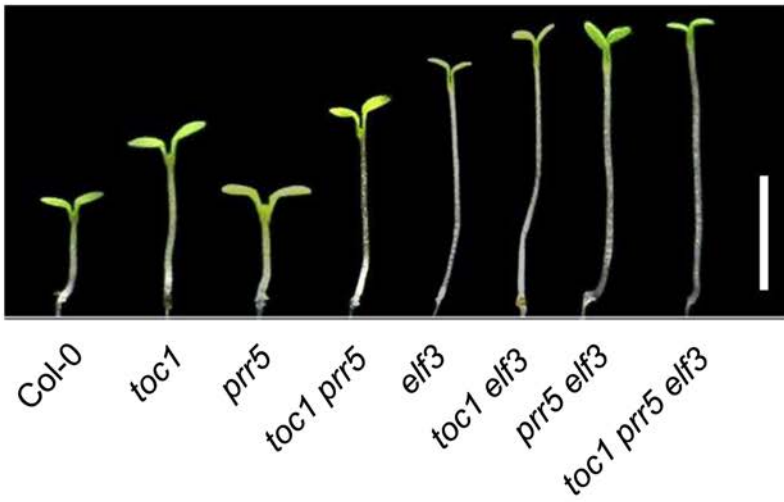
852 **Yanovsky MJ, Kay SA** (2002) Molecular basis of seasonal time measurement in *Arabidopsis*.
853 *Nature* **419**: 308-312

854 **Zhang Y, Wang Y, Wei H, Li N, Tian W, Chong K, Wang L** (2018) Circadian Evening
855 Complex Represses Jasmonate-Induced Leaf Senescence in *Arabidopsis*. *Mol Plant* **11**:
856 326-337

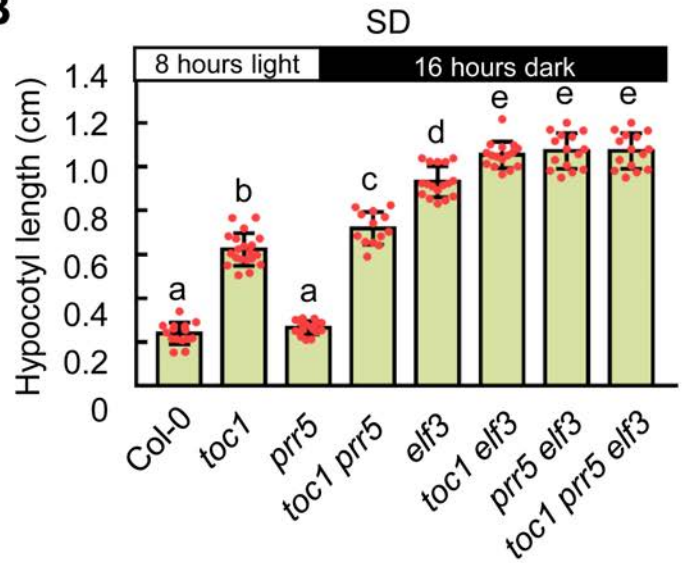
857 **Zhu JY, Oh E, Wang T, Wang ZY** (2016) TOC1-PIF4 interaction mediates the circadian
858 gating of thermoresponsive growth in *Arabidopsis*. *Nat Commun* **7**: 13692

859

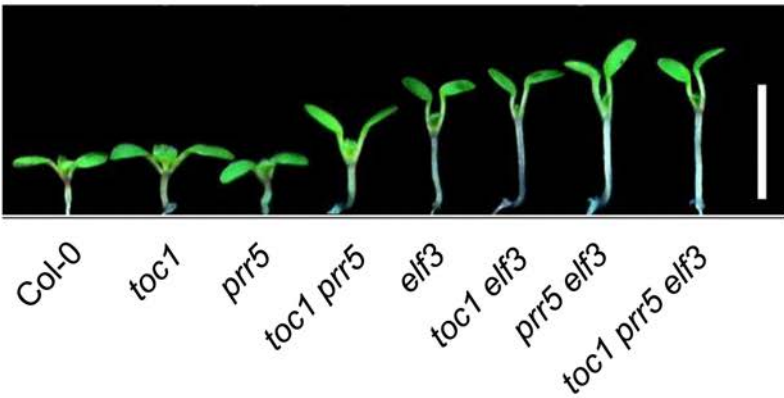
A In short day (SD)



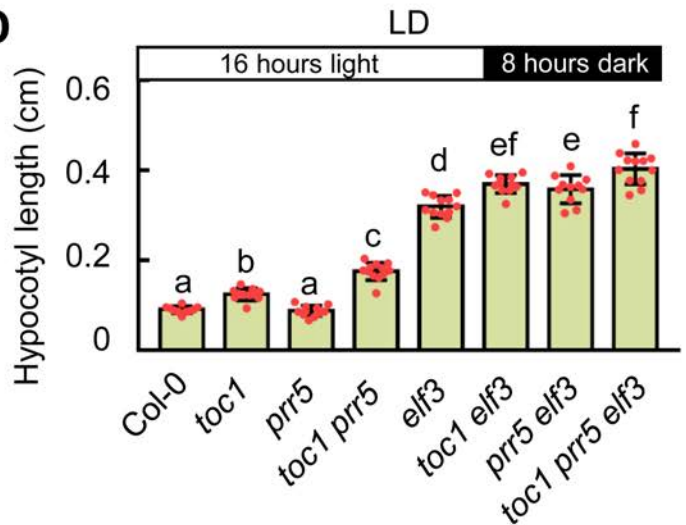
B



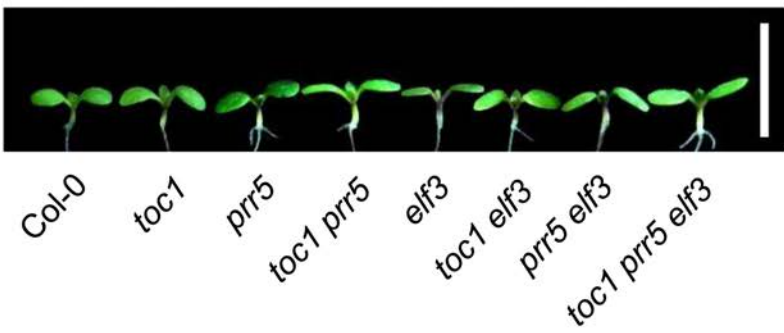
C In long day (LD)



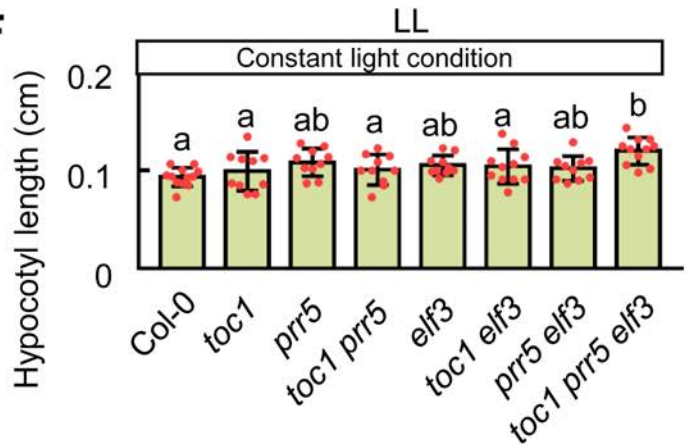
D

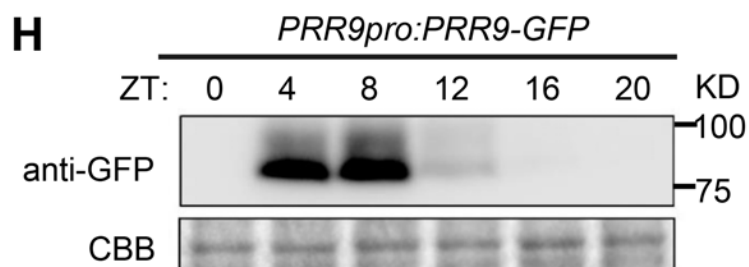
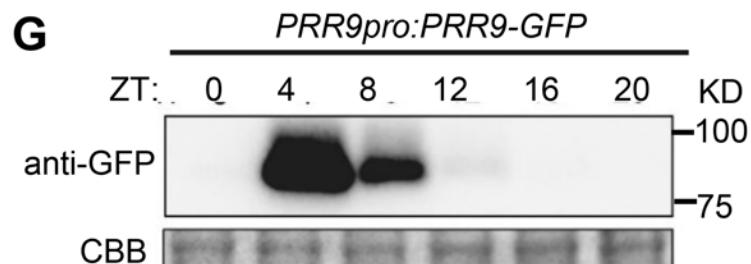
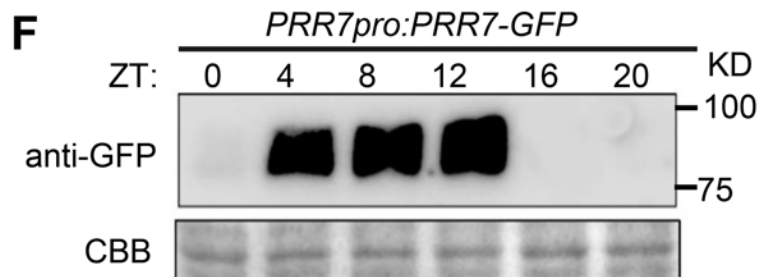
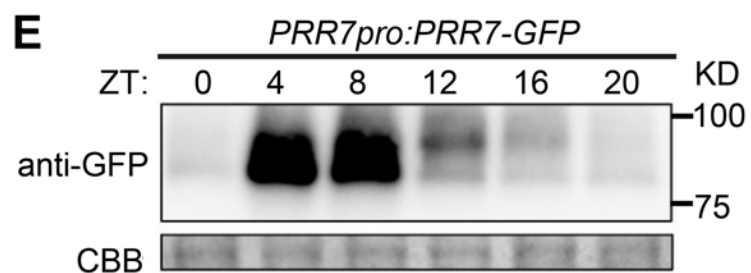
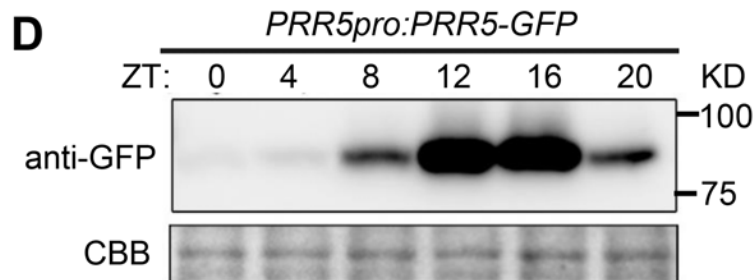
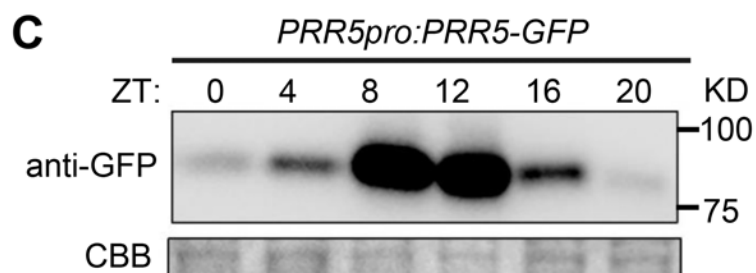
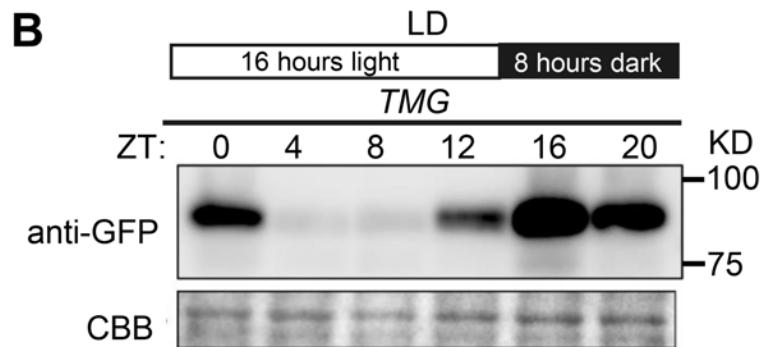
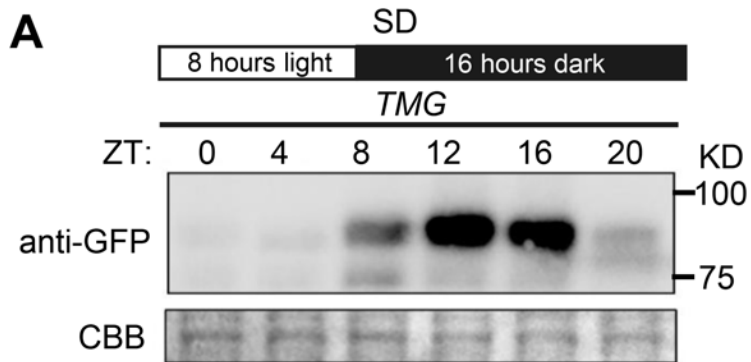


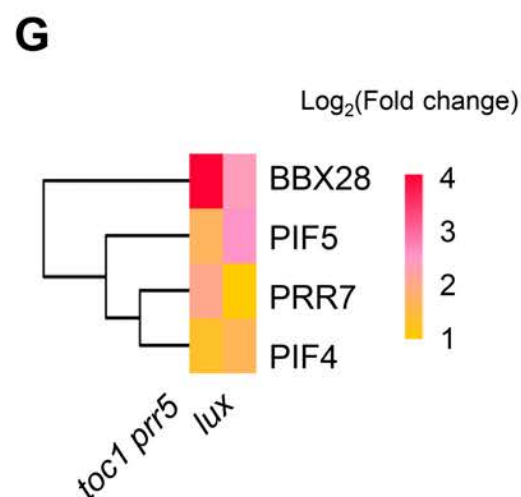
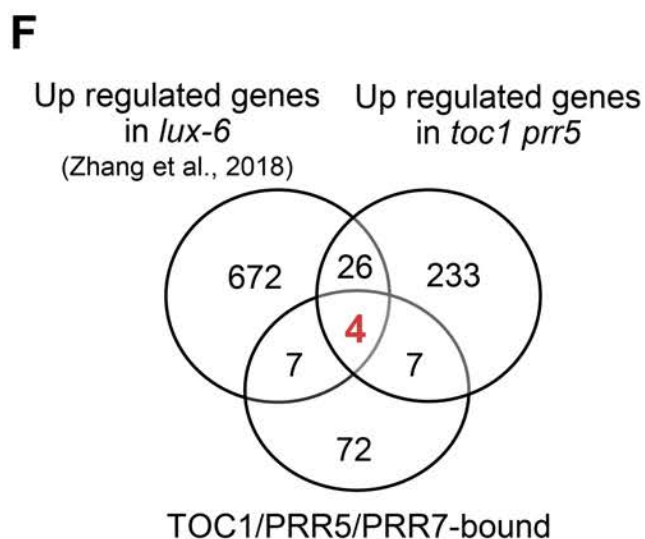
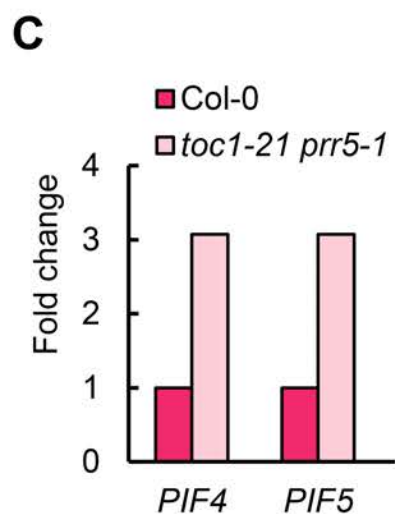
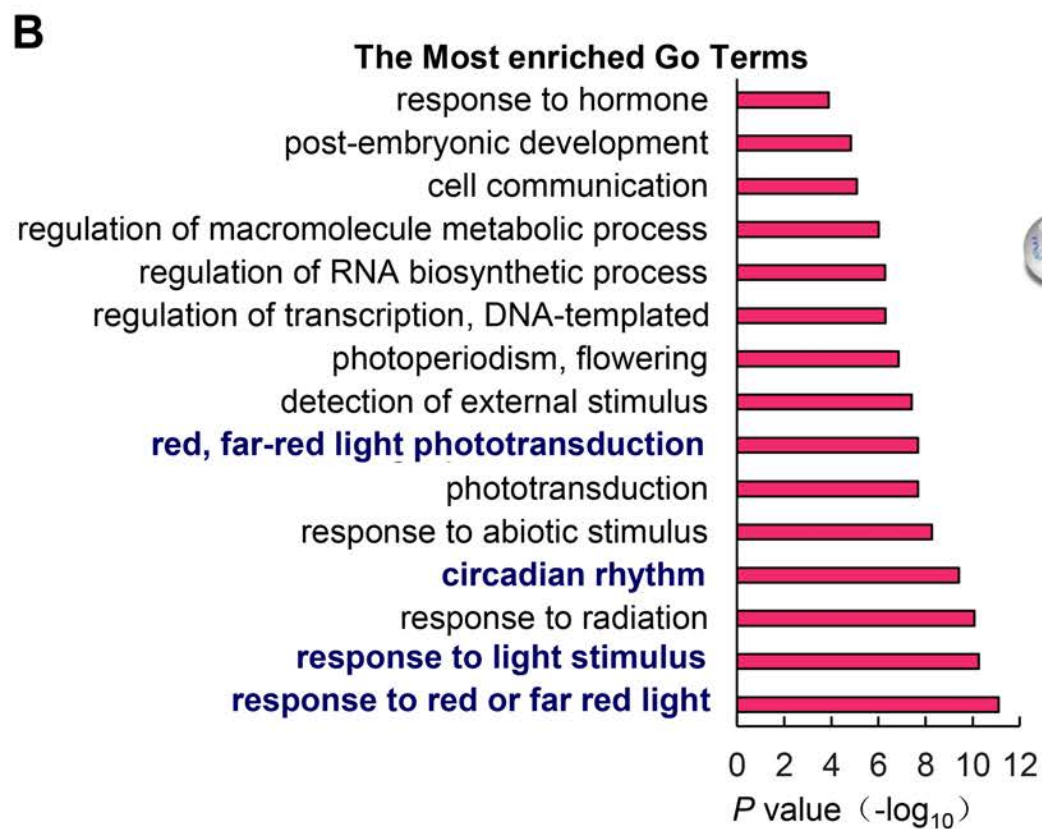
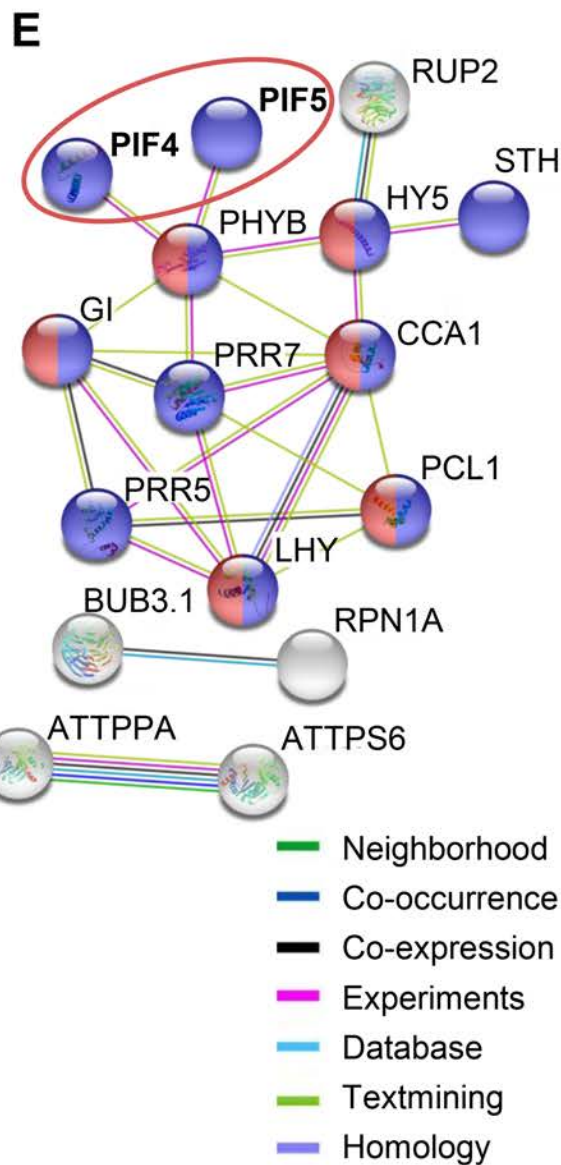
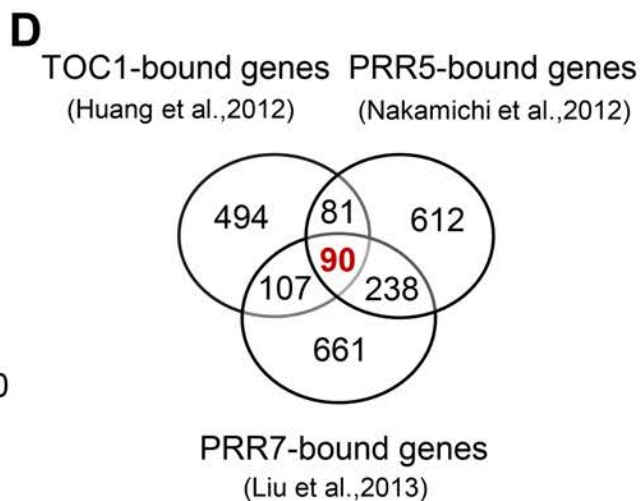
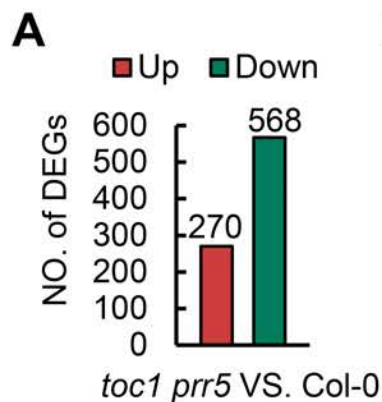
E In constant light (LL)

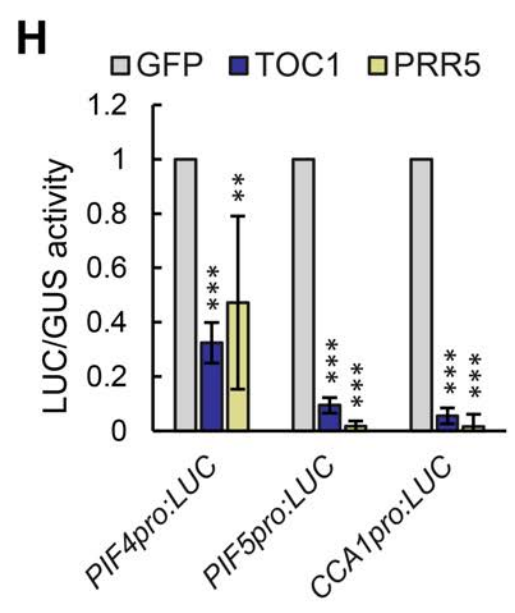
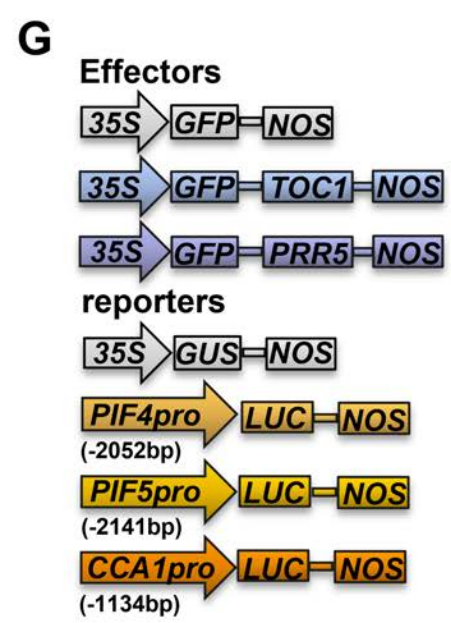
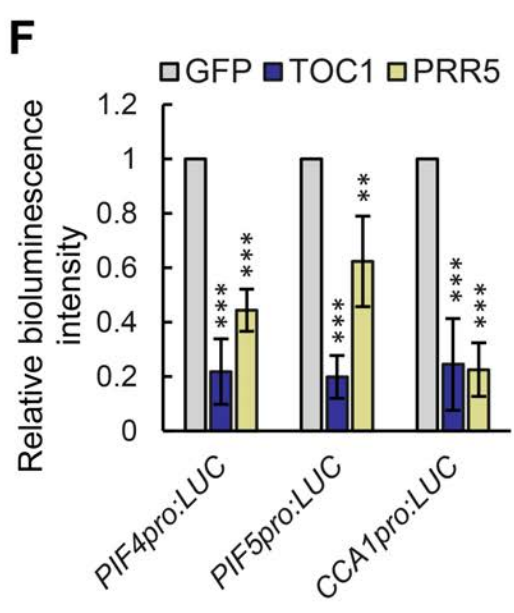
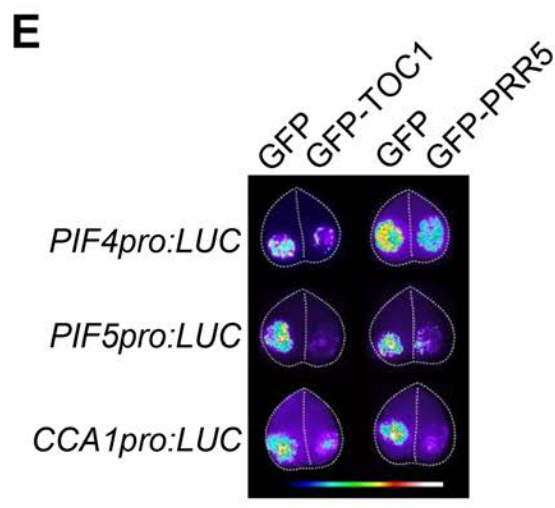
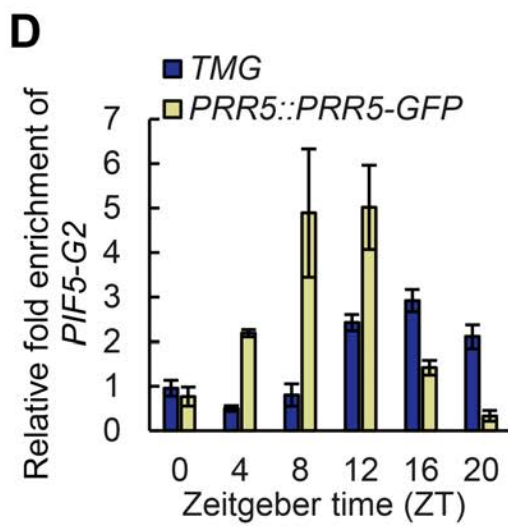
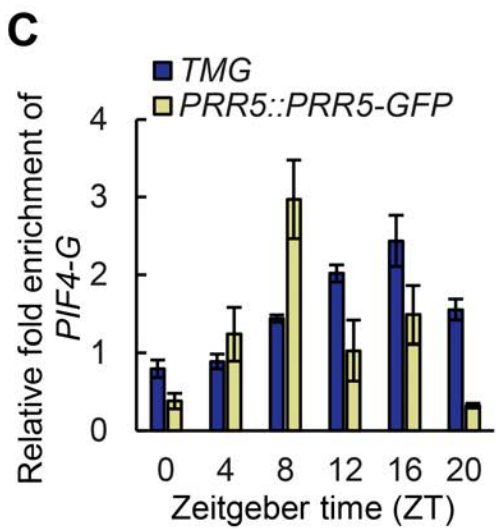
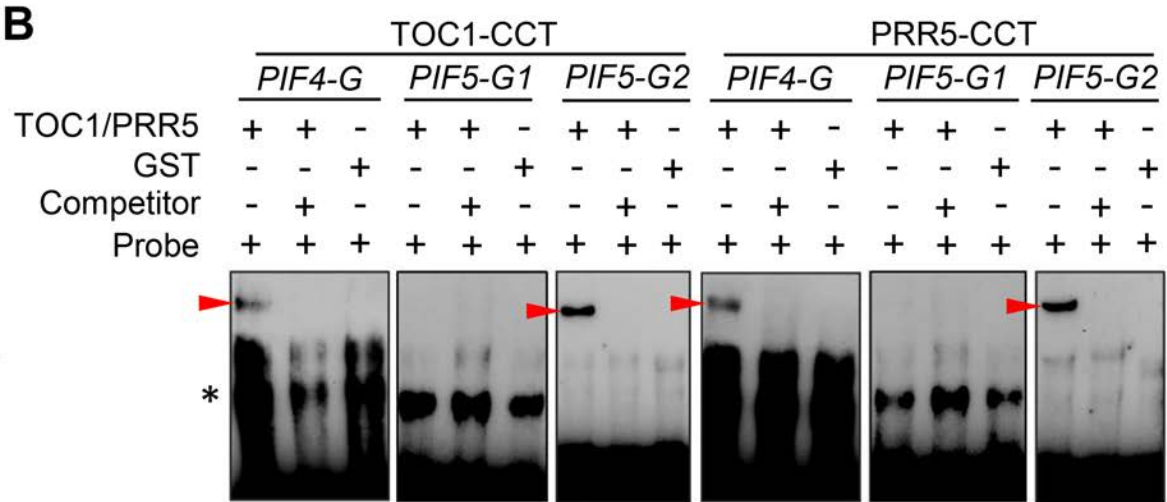
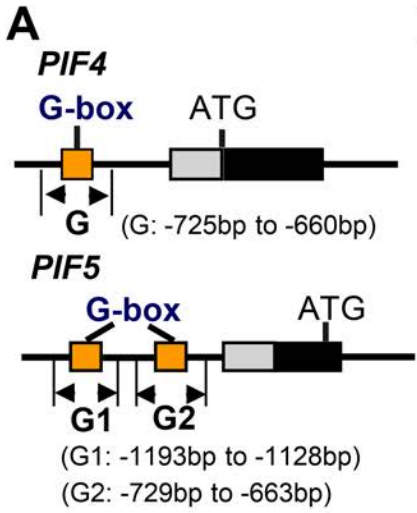


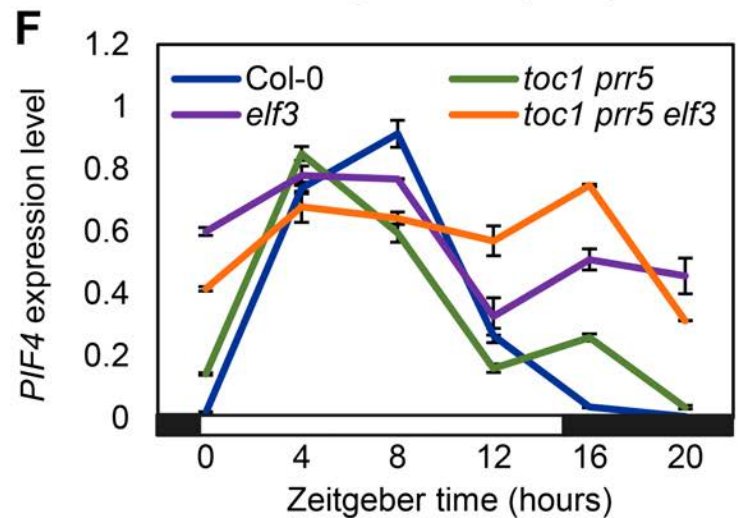
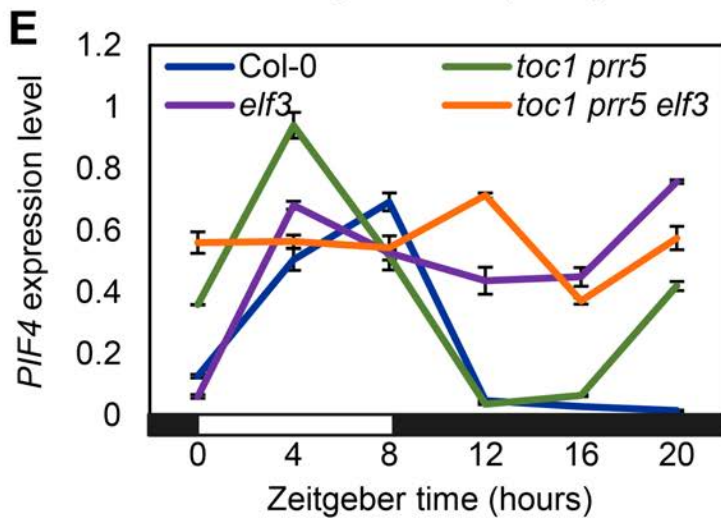
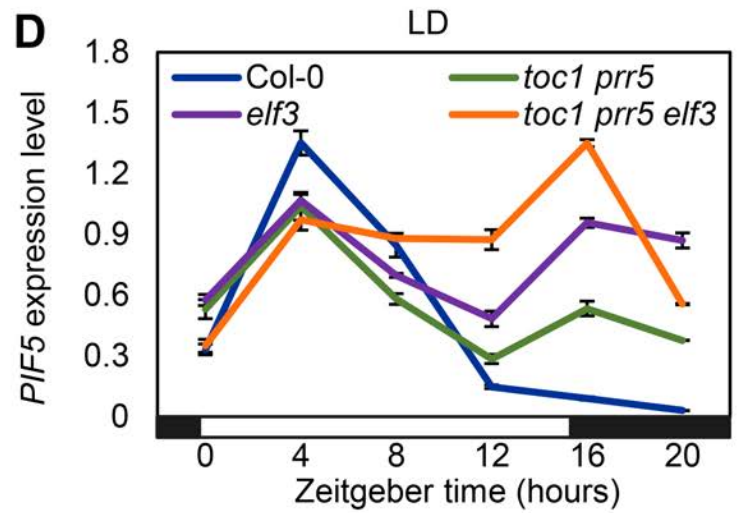
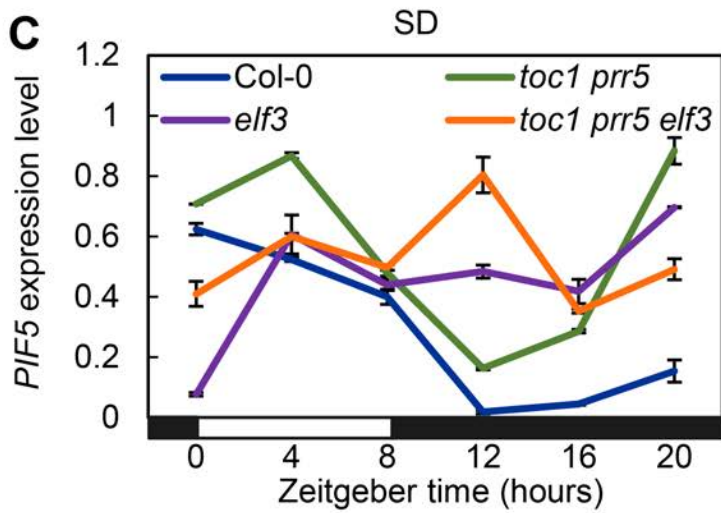
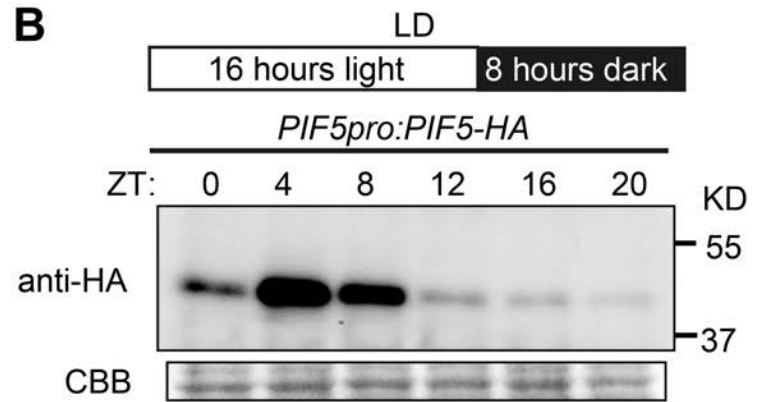
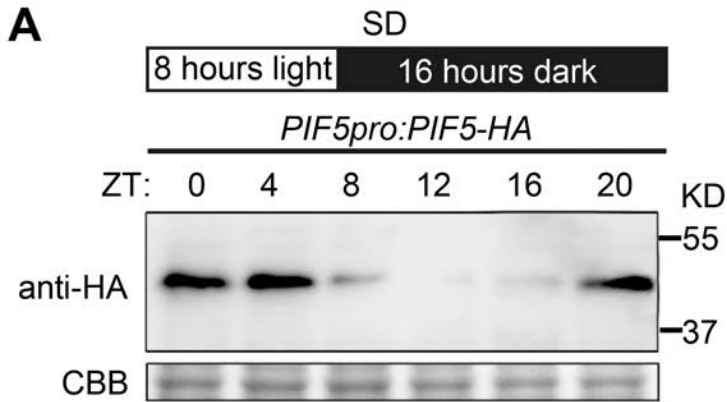
F

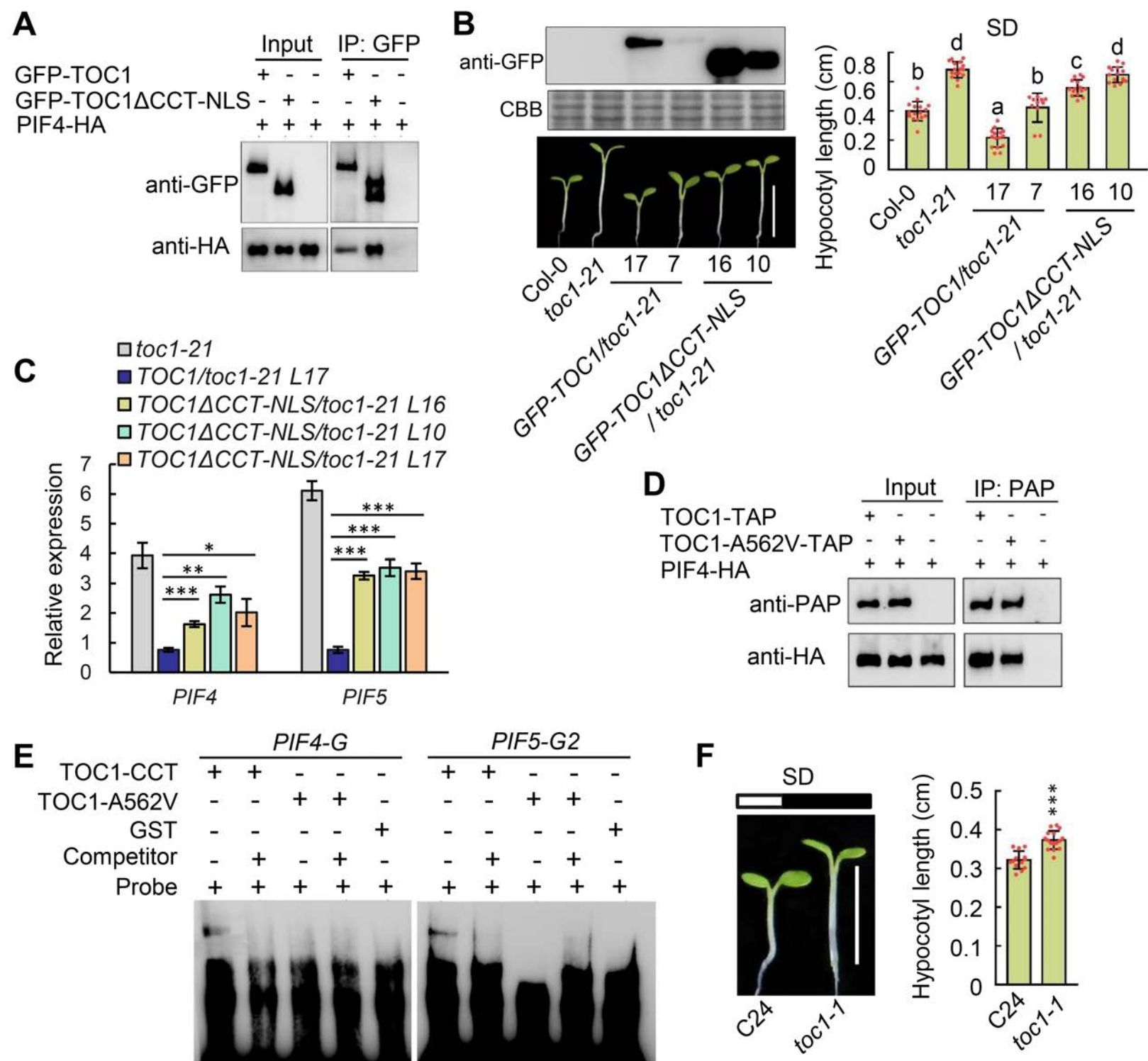


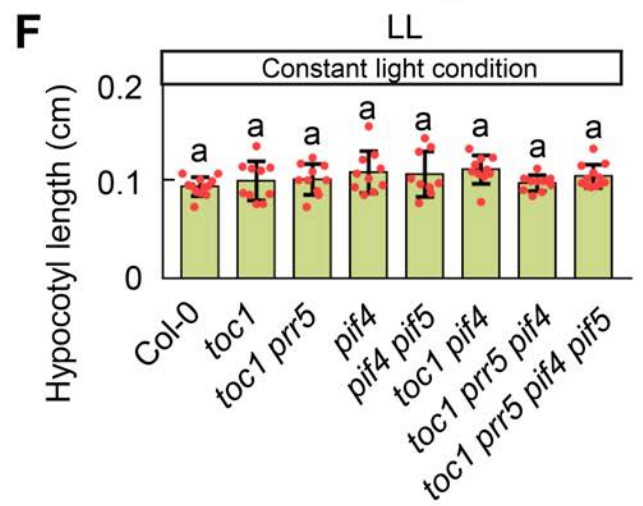
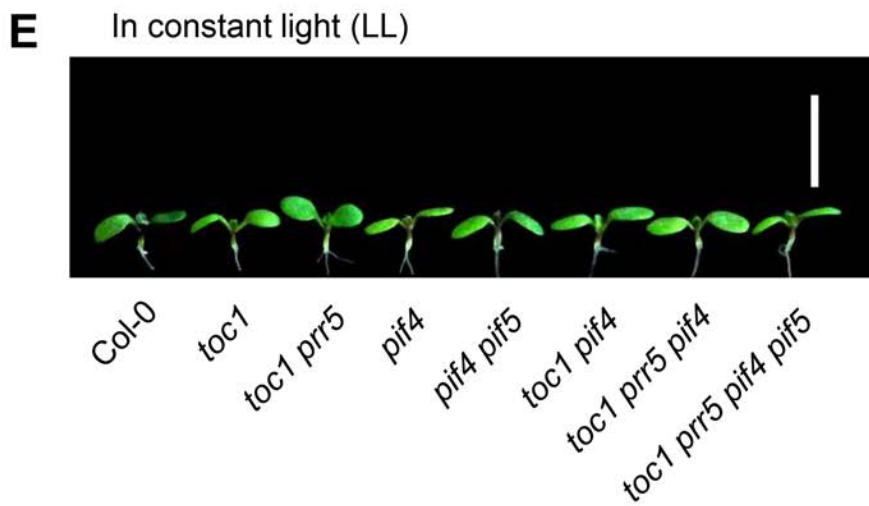
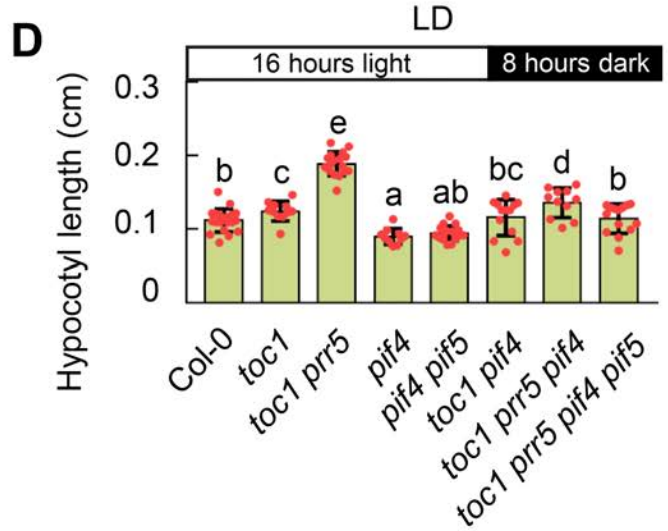
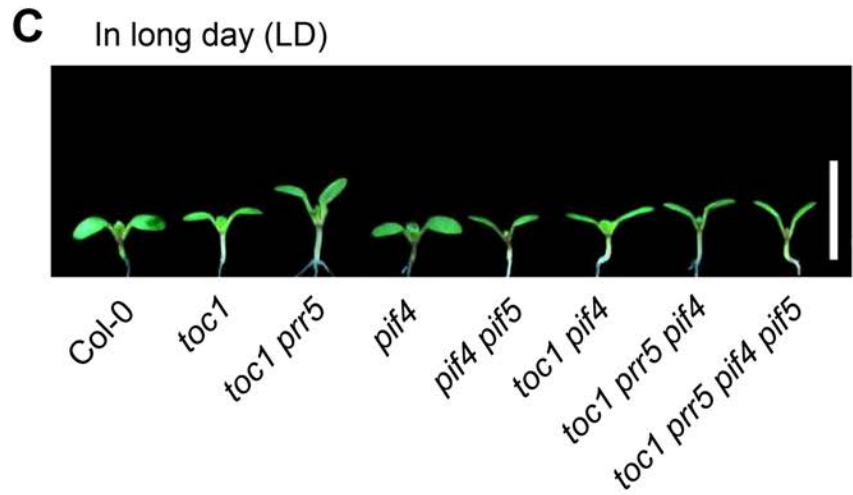
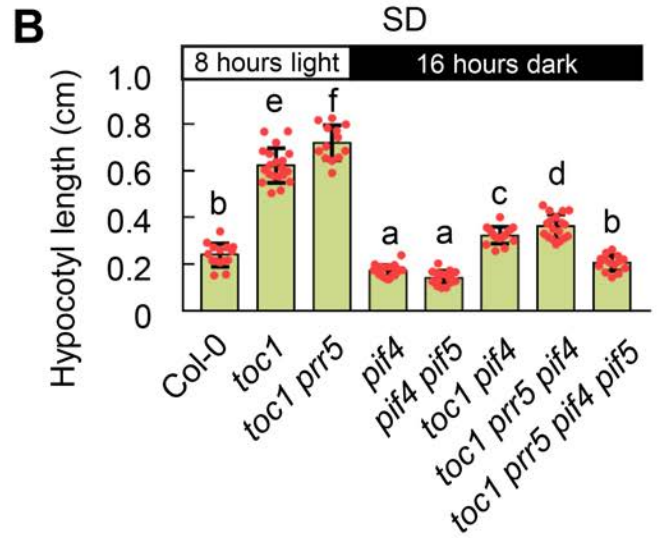
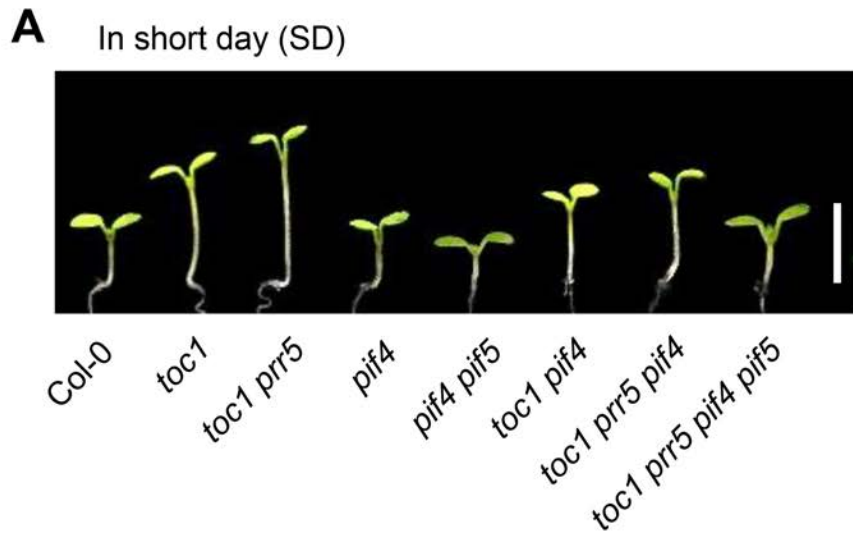




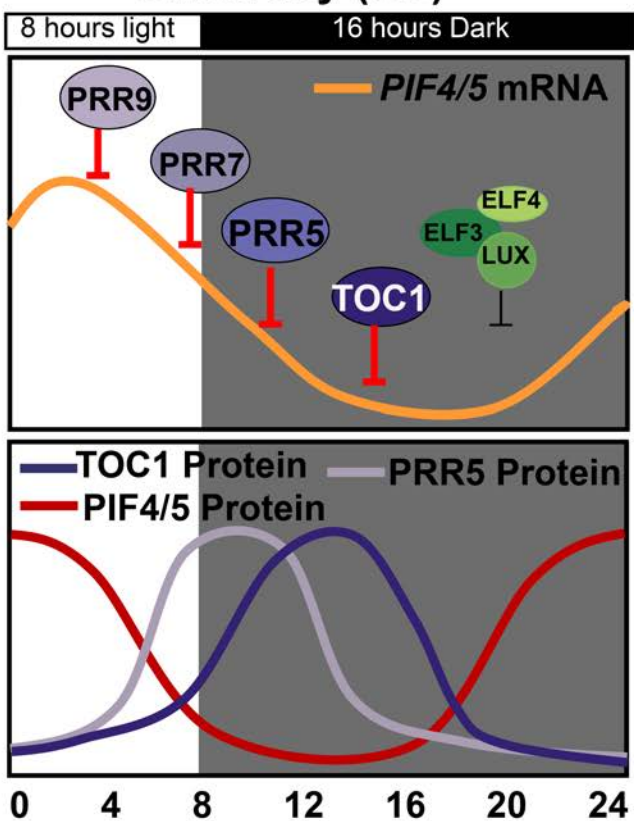




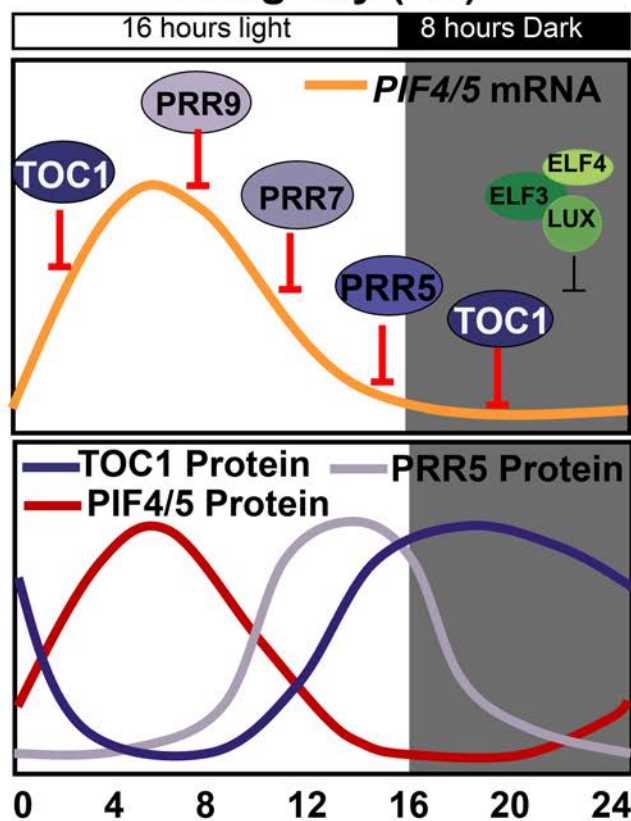




Short day (SD)



Long day (LD)



Parsed Citations

Al-Sady B, Ni W, Kircher S, Schafer E, Quail PH (2006) Photoactivated phytochrome induces rapid PIF3 phosphorylation prior to proteasome-mediated degradation. *Mol Cell* 23: 439-446

Pubmed: [Author and Title](#)

Google Scholar: [Author Only Title Only Author and Title](#)

Andres F, Coupland G (2012) The genetic basis of flowering responses to seasonal cues. *Nat Rev Genet* 13: 627-639

Pubmed: [Author and Title](#)

Google Scholar: [Author Only Title Only Author and Title](#)

Dowson-Day MJ, Millar AJ (1999) Circadian dysfunction causes aberrant hypocotyl elongation patterns in *Arabidopsis*. *Plant J* 17: 63-71

Pubmed: [Author and Title](#)

Google Scholar: [Author Only Title Only Author and Title](#)

Ding Z, Doyle MR, Amasino RM, Davis SJ (2007) A complex genetic interaction between *Arabidopsis thaliana* TOC1 and CCA1/LHY in driving the circadian clock and in output regulation. *Genetics* 176: 1501-1510

Pubmed: [Author and Title](#)

Google Scholar: [Author Only Title Only Author and Title](#)

Fujimori T, Yamashino T, Kato T, Mizuno T (2004) Circadian-controlled basic/helix-loop-helix factor, PIL6, implicated in light-signal transduction in *Arabidopsis thaliana*. *Plant Cell Physiol* 45: 1078-1086

Pubmed: [Author and Title](#)

Google Scholar: [Author Only Title Only Author and Title](#)

Fujiwara S, Wang L, Han L, Suh SS, Salome PA, McClung CR, Somers DE (2008) Post-translational regulation of the *Arabidopsis* circadian clock through selective proteolysis and phosphorylation of pseudo-response regulator proteins. *J Biol Chem* 283: 23073-23083

Pubmed: [Author and Title](#)

Google Scholar: [Author Only Title Only Author and Title](#)

Gendron JM, Pruneda-Paz JL, Doherty CJ, Gross AM, Kang SE, Kay SA (2012) *Arabidopsis* circadian clock protein, TOC1, is a DNA-binding transcription factor. *Proc Natl Acad Sci USA* 109: 3167-3172

Pubmed: [Author and Title](#)

Google Scholar: [Author Only Title Only Author and Title](#)

Hazen SP, Schultz TF, Pruneda-Paz JL, Borevitz JO, Ecker JR, Kay SA (2005) LUX ARRHYTHMO encodes a Myb domain protein essential for circadian rhythms. *Proc Natl Acad Sci USA* 102: 10387-10392

Pubmed: [Author and Title](#)

Google Scholar: [Author Only Title Only Author and Title](#)

Huang H, Alvarez S, Bindbeutel R, Shen Z, Naldrett MJ, Evans BS, Briggs SP, Hicks LM, Kay SA, Nusinow DA (2016) Identification of Evening Complex Associated Proteins in *Arabidopsis* by Affinity Purification and Mass Spectrometry. *Mol Cell Proteomics* 15: 201-217

Pubmed: [Author and Title](#)

Google Scholar: [Author Only Title Only Author and Title](#)

Huang W, Perez-Garcia P, Pokhilko A, Millar AJ, Antoshechkin I, Riechmann JL, Mas P (2012) Mapping the core of the *Arabidopsis* circadian clock defines the network structure of the oscillator. *Science* 336: 75-79

Pubmed: [Author and Title](#)

Google Scholar: [Author Only Title Only Author and Title](#)

Huq E, Quail PH (2002) PIF4, a phytochrome-interacting bHLH factor, functions as a negative regulator of phytochrome B signaling in *Arabidopsis*. *EMBO J* 21: 2441-2450

Pubmed: [Author and Title](#)

Google Scholar: [Author Only Title Only Author and Title](#)

Kaczorowski KA, Quail PH (2003) *Arabidopsis* PSEUDO-RESPONSE REGULATOR7 is a signaling intermediate in phytochrome-regulated seedling deetiolation and phasing of the circadian clock. *Plant Cell* 15: 2654-2665

Pubmed: [Author and Title](#)

Google Scholar: [Author Only Title Only Author and Title](#)

Lee BD, Kim MR, Kang MY, Cha JY, Han SH, Nawkar GM, Sakuraba Y, Lee SY, Imaizumi T, McClung CR, Kim WY, Paek NC (2017) The F-box protein FKF1 inhibits dimerization of COP1 in the control of photoperiodic flowering. *Nat Commun* 8: 2259

Pubmed: [Author and Title](#)

Google Scholar: [Author Only Title Only Author and Title](#)

Leivar P, Monte E, Al-Sady B, Carle C, Storer A, Alonso JM, Ecker JR, Quail PH (2008) The *Arabidopsis* phytochrome-interacting factor PIF7, together with PIF3 and PIF4, regulates responses to prolonged red light by modulating phyB levels. *Plant Cell* 20: 337-352

Pubmed: [Author and Title](#)

Google Scholar: [Author Only Title Only Author and Title](#)

Li B, Wang Y, Zhang Y, Tian W, Chong K, Jang JC, and Wang L (2019) PRR5, 7 and 9 positively modulate TOR signaling-mediated root cell proliferation by repressing TANDEM ZINC FINGER 1 in *Arabidopsis*. *Nucleic Acids Res* 47:5001-5015.

Pubmed: [Author and Title](#)

Downloaded from on March 24, 2020 - Published by www.plantphysiol.org
Copyright © 2020 American Society of Plant Biologists. All rights reserved.

Google Scholar: [Author Only](#) [Title Only](#) [Author and Title](#)

Liu T, Carlsson J, Takeuchi T, Newton L, Farre EM (2013) Direct regulation of abiotic responses by the Arabidopsis circadian clock component PRR7. Plant J 76: 101-114

Pubmed: [Author and Title](#)

Google Scholar: [Author Only](#) [Title Only](#) [Author and Title](#)

Liu TL, Newton L, Liu MJ, Shiu SH, Farre EM (2016) A G-Box-Like Motif Is Necessary for Transcriptional Regulation by Circadian Pseudo-Response Regulators in Arabidopsis. Plant Physiol 170: 528-539

Pubmed: [Author and Title](#)

Google Scholar: [Author Only](#) [Title Only](#) [Author and Title](#)

Ma D, Li X, Guo Y, Chu J, Fang S, Yan C, Noel JP, Liu H (2016) Cryptochrome 1 interacts with PIF4 to regulate high temperature-mediated hypocotyl elongation in response to blue light. Proc Natl Acad Sci USA 113: 224-229

Pubmed: [Author and Title](#)

Google Scholar: [Author Only](#) [Title Only](#) [Author and Title](#)

Martin G, Rovira A, Veciana N, Soy J, Toledo-Ortiz G, Gommers CMM, Boix M, Henriques R, Minguet EG, Alabadi D, Halliday KJ, Leivar P, Monte E (2018) Circadian Waves of Transcriptional Repression Shape PIF-Regulated Photoperiod-Responsive Growth in Arabidopsis. Curr Biol 28: 311-318 e315

Pubmed: [Author and Title](#)

Google Scholar: [Author Only](#) [Title Only](#) [Author and Title](#)

Mas P, Kim WY, Somers DE, Kay SA (2003) Targeted degradation of TOC1 by ZTL modulates circadian function in Arabidopsis thaliana. Nature 426: 567-570

Pubmed: [Author and Title](#)

Google Scholar: [Author Only](#) [Title Only](#) [Author and Title](#)

Matsushika A, Makino S, Kojima M, Mizuno T (2000) Circadian waves of expression of the APRR1/TOC1 family of pseudo-response regulators in Arabidopsis thaliana: insight into the plant circadian clock. Plant Cell Physiol 41: 1002-1012

Pubmed: [Author and Title](#)

Google Scholar: [Author Only](#) [Title Only](#) [Author and Title](#)

Millar AJ (2016) The Intracellular Dynamics of Circadian Clocks Reach for the Light of Ecology and Evolution. Annu Rev Plant Biol 67: 595-618

Pubmed: [Author and Title](#)

Google Scholar: [Author Only](#) [Title Only](#) [Author and Title](#)

Nakamichi N, Kiba T, Henriques R, Mizuno T, Chua NH, Sakakibara H (2010) PSEUDO-RESPONSE REGULATORS 9, 7, and 5 are transcriptional repressors in the Arabidopsis circadian clock. Plant Cell 22: 594-605

Pubmed: [Author and Title](#)

Google Scholar: [Author Only](#) [Title Only](#) [Author and Title](#)

Nakamichi N, Kiba T, Kamioka M, Suzuki T, Yamashino T, Higashiyama T, Sakakibara H, Mizuno T (2012) Transcriptional repressor PRR5 directly regulates clock-output pathways. Proc Natl Acad Sci USA 109: 17123-17128

Pubmed: [Author and Title](#)

Google Scholar: [Author Only](#) [Title Only](#) [Author and Title](#)

Nakamichi N, Kita M, Ito S, Yamashino T, Mizuno T (2005) PSEUDO-RESPONSE REGULATORS, PRR9, PRR7 and PRR5, together play essential roles close to the circadian clock of Arabidopsis thaliana. Plant Cell Physiol 46: 686-698

Pubmed: [Author and Title](#)

Google Scholar: [Author Only](#) [Title Only](#) [Author and Title](#)

Nieto C, Lopez-Salmeron V, Daviere JM, Prat S (2015) ELF3-PIF4 interaction regulates plant growth independently of the Evening Complex. Curr Biol 25: 187-193

Pubmed: [Author and Title](#)

Google Scholar: [Author Only](#) [Title Only](#) [Author and Title](#)

Niwa Y, Yamashino T, Mizuno T (2009) The circadian clock regulates the photoperiodic response of hypocotyl elongation through a coincidence mechanism in Arabidopsis thaliana. Plant Cell Physiol 50: 838-854

Pubmed: [Author and Title](#)

Google Scholar: [Author Only](#) [Title Only](#) [Author and Title](#)

Nohales MA, Liu W, Duffy T, Nozue K, Sawa M, Pruneda-Paz JL, Maloof JN, Jacobsen SE, Kay SA (2019) Multi-level Modulation of Light Signaling by GIGANTEA Regulates Both the Output and Pace of the Circadian Clock. Dev Cell 49: 840-851 e848

Pubmed: [Author and Title](#)

Google Scholar: [Author Only](#) [Title Only](#) [Author and Title](#)

Nomoto Y, Kubozono S, Miyachi M, Yamashino T, Nakamichi N, Mizuno T (2012) A circadian clock- and PIF4-mediated double coincidence mechanism is implicated in the thermosensitive photoperiodic control of plant architectures in Arabidopsis thaliana. Plant Cell Physiol 53: 1965-1973

Pubmed: [Author and Title](#)

Google Scholar: [Author Only](#) [Title Only](#) [Author and Title](#)

Nozue K, Covington MF, Duek PD, Loraire S, Frankhauser Q, Hanzel P, Slight M, Maloof JN (2007) Rhythmic growth explained by coincidence

between internal and external cues. *Nature* 448: 358-361

Pubmed: [Author and Title](#)

Google Scholar: [Author Only Title Only Author and Title](#)

Nusinow DA, Helfer A, Hamilton EE, King JJ, Imaizumi T, Schultz TF, Farre EM, Kay SA (2011) The ELF4-ELF3-LUX complex links the circadian clock to diurnal control of hypocotyl growth. *Nature* 475: 398-402

Pubmed: [Author and Title](#)

Google Scholar: [Author Only Title Only Author and Title](#)

Pedmale UV, Huang SC, Zander M, Cole BJ, Hetzel J, Ljung K, Reis PAB, Sridevi P, Nito K, Nery JR, Ecker JR, Chory J (2016) Cryptochromes Interact Directly with PIFs to Control Plant Growth in Limiting Blue Light. *Cell* 164: 233-245

Pubmed: [Author and Title](#)

Google Scholar: [Author Only Title Only Author and Title](#)

Quint M, Delker C, Franklin KA, Wigge PA, Halliday KJ, van Zanten M (2016) Molecular and genetic control of plant thermomorphogenesis. *Nat Plants* 2: 15190

Pubmed: [Author and Title](#)

Google Scholar: [Author Only Title Only Author and Title](#)

Sakuraba Y, Jeong J, Kang MY, Kim J, Paek NC, Choi G (2014) Phytochrome-interacting transcription factors PIF4 and PIF5 induce leaf senescence in *Arabidopsis*. *Nat Commun* 5: 4636

Pubmed: [Author and Title](#)

Google Scholar: [Author Only Title Only Author and Title](#)

Sanchez SE, Kay SA (2016) The Plant Circadian Clock: From a Simple Timekeeper to a Complex Developmental Manager. *Cold Spring Harb Perspect Biol* 8: a027748

Pubmed: [Author and Title](#)

Google Scholar: [Author Only Title Only Author and Title](#)

Sato E, Nakamichi N, Yamashino T, Mizuno T (2002) Aberrant expression of the *Arabidopsis* circadian-regulated APRR5 gene belonging to the APRR1/TOC1 quintet results in early flowering and hypersensitiveness to light in early photomorphogenesis. *Plant Cell Physiol* 43: 1374-1385

Pubmed: [Author and Title](#)

Google Scholar: [Author Only Title Only Author and Title](#)

Sawa M, Kay SA (2011) GIGANTEA directly activates Flowering Locus T in *Arabidopsis thaliana*. *Proc Natl Acad Sci USA* 108: 11698-11703

Pubmed: [Author and Title](#)

Google Scholar: [Author Only Title Only Author and Title](#)

Sawa M, Nusinow DA, Kay SA, Imaizumi T (2007) FKF1 and GIGANTEA complex formation is required for day-length measurement in *Arabidopsis*. *Science* 318: 261-265

Pubmed: [Author and Title](#)

Google Scholar: [Author Only Title Only Author and Title](#)

Shen Y, Khanna R, Carle CM, Quail PH (2007) Phytochrome induces rapid PIF5 phosphorylation and degradation in response to red-light activation. *Plant Physiol* 145: 1043-1051

Pubmed: [Author and Title](#)

Google Scholar: [Author Only Title Only Author and Title](#)

Song Y, Yang C, Gao S, Zhang W, Li L, Kuai B (2014) Age-triggered and dark-induced leaf senescence require the bHLH transcription factors PIF3, 4, and 5. *Mol Plant* 7: 1776-1787

Pubmed: [Author and Title](#)

Google Scholar: [Author Only Title Only Author and Title](#)

Song YH, Smith RW, To BJ, Millar AJ, Imaizumi T (2012) FKF1 conveys timing information for CONSTANS stabilization in photoperiodic flowering. *Science* 336: 1045-1049

Pubmed: [Author and Title](#)

Google Scholar: [Author Only Title Only Author and Title](#)

Soy J, Leivar P, Gonzalez-Schain N, Martin G, Diaz C, Sentandreu M, Al-Sady B, Quail PH, Monte E (2016) Molecular convergence of clock and photosensory pathways through PIF3-TOC1 interaction and co-occupancy of target promoters. *Proc Natl Acad Sci USA* 113: 4870-4875

Pubmed: [Author and Title](#)

Google Scholar: [Author Only Title Only Author and Title](#)

Strayer C, Oyama T, Schultz TF, Raman R, Somers DE, Mas P, Panda S, Kreps JA, Kay SA (2000) Cloning of the *Arabidopsis* clock gene TOC1, an autoregulatory response regulator homolog. *Science* 289: 768-771

Pubmed: [Author and Title](#)

Google Scholar: [Author Only Title Only Author and Title](#)

Sun Q, Wang S, Xu G, Kang X, Zhang M, Ni M (2019) SHB1 and CCA1 interaction desensitizes light responses and enhances thermomorphogenesis. *Nat Commun* 10: 3110

Pubmed: [Author and Title](#)

Google Scholar: [Author Only Title Only Author and Title](#)

Valverde F, Mouradov A, Soppe W, Ravenscroft D, Samach A, Coupland G (2004) Photoreceptor regulation of CONSTANS protein in photoperiodic flowering. Science 303: 1003-1006

Pubmed: [Author and Title](#)

Google Scholar: [Author Only Title Only Author and Title](#)

Wang L, Fujiwara S, Somers DE (2010) PRR5 regulates phosphorylation, nuclear import and subnuclear localization of TOC1 in the Arabidopsis circadian clock. EMBO J 29: 1903-1915

Pubmed: [Author and Title](#)

Google Scholar: [Author Only Title Only Author and Title](#)

Yamamoto Y, Sato E, Shimizu T, Nakamichi N, Sato S, Kato T, Tabata S, Nagatani A, Yamashino T, Mizuno T (2003) Comparative genetic studies on the APRR5 and APRR7 genes belonging to the APRR1/TOC1 quintet implicated in circadian rhythm, control of flowering time, and early photomorphogenesis. Plant Cell Physiol 44: 1119-1130

Pubmed: [Author and Title](#)

Google Scholar: [Author Only Title Only Author and Title](#)

Yamashino T, Ito S, Niwa Y, Kunihiro A, Nakamichi N, Mizuno T (2008) Involvement of Arabidopsis clock-associated pseudo-response regulators in diurnal oscillations of gene expression in the presence of environmental time cues. Plant Cell Physiol 49: 1839-1850

Pubmed: [Author and Title](#)

Google Scholar: [Author Only Title Only Author and Title](#)

Yanovsky MJ, Kay SA (2002) Molecular basis of seasonal time measurement in Arabidopsis. Nature 419: 308-312

Pubmed: [Author and Title](#)

Google Scholar: [Author Only Title Only Author and Title](#)

Zhang Y, Wang Y, Wei H, Li N, Tian W, Chong K, Wang L (2018) Circadian Evening Complex Represses Jasmonate-Induced Leaf Senescence in Arabidopsis. Mol Plant 11: 326-337

Pubmed: [Author and Title](#)

Google Scholar: [Author Only Title Only Author and Title](#)

Zhu JY, Oh E, Wang T, Wang ZY (2016) TOC1-PIF4 interaction mediates the circadian gating of thermoresponsive growth in Arabidopsis. Nat Commun 7: 13692

Pubmed: [Author and Title](#)

Google Scholar: [Author Only Title Only Author and Title](#)